RESEARCH ARTICLE | SEPTEMBER 23 2025

Geometric potential for a Bose–Einstein condensate on a curved surface

Special Collection: Quantum Bubbles

Sheilla M. de Oliveira ; Natália Salomé Móller

AVS Quantum Sci. 7, 033203 (2025)
https://doi.org/10.1116/5.0281991

Geometric potential for a Bose–Einstein condensate on a curved surface

Cite as: AVS Quantum Sci. 7, 033203 (2025); doi: 10.1116/5.0281991
Submitted: 22 May 2025 · Accepted: 28 August 2025 ·
Published Online: 23 September 2025

Sheilla M. de Oliveira[1,2] and Natália Salomé Móller[3,a)]

AFFILIATIONS

[1]Physics Department and Research Center OPTIMAS, Rhineland-Palatinate Technical University Kaiserslautern-Landau, Erwin-Schrödinger Straße 46, 67663 Kaiserslautern, Germany
[2]Instituto de Física de São Carlos, Universidade de São Paulo, 13566-590 São Carlos, SP, Brazil
[3]Research Center for Quantum Information, Institute of Physics, Slovak Academy of Sciences, Dúbravská Cesta 9, 84511 Bratislava, Slovakia

Note: This paper is part of the special issue on Quantum Bubbles.
[a)]**Electronic mail:** natalia.moller@savba.sk

ABSTRACT

We compute the ground state of a Bose–Einstein condensate confined on a curved surface and unravel the effects of curvatures. Starting with a general formulation for any smooth surface, we apply it to a prolate ellipsoid, which is inspired by recent bubble trap experiments. Using only elementary tools, we perform a perturbative approach to the Gross–Pitaevskii equation and a general Ansatz, followed by a dimensional reduction. We derive an effective two-dimensional equation that includes a curvature-dependent geometric potential. We compute the ground state using the Thomas–Fermi approximation and, for an isotropic confinement, we find that the highest accumulation of atoms happens in the regions with the greatest difference between the principal curvatures. For a prolate ellipsoid, this accumulation happens on the equator, which is contrary to previous findings that describe accumulation on the poles of a bubble trap. Finally, we explain the reasons for this difference: the higher accumulation of atoms on the poles happens due to anisotropies in the confinement, while the higher accumulation on the equator happens exclusively due to the geometric properties of the surface.

I. INTRODUCTION

The physics of quantum systems constrained to curved manifolds of one- and two-dimensions was already the subject of interest in the last century, where effective low-dimensional Schröndinger equations were derived.[1–3] Dimensional reduction techniques have found application in diverse fields, such as in electronic materials,[4,5] photonics,[6] and DNA wires.[7] Of particular relevance to the present work, there is a variety of results of Bose–Einstein condensates (BECs) on curved wires and surfaces.[8]

Flat geometries are particular cases of curved geometries, where the curvatures vanish everywhere. Experiments of BECs on flat manifolds of one and two dimensions have already been performed by many groups with diverse techniques,[9] where cigar-shaped and disk-shaped traps are realized.[10,11] Curiously, it was initially believed to not be possible to implement a BEC on low dimensions, due to the Hohenberg–Mermin–Wagner theorem that predicts that the phase transition to a BEC happens only at null temperature in a homogeneous system.[12,13] Later, it was found that different boundary conditions for a low-dimensional flat trap allow the BEC formation at a positive temperature.[14] Theoretical dimensional reduction techniques for these flat traps can be found, for instance, in Refs. 15–18.

The confinement of BECs on one-dimensional curved manifolds has already been experimentally demonstrated as well, where ring-shaped potentials have been quite often explored.[19–25] To cite a few applications, one can characterize the rotation of a ring,[26] its employment on atomtronics,[27] the propagation of solitons[28] and sound waves,[29] and even the simulation of an early universe in expansion.[30] Ring-shaped traps are one specific kind of curved manifold with the shape of a circular ring. One can also find the demonstration of more exotic shapes of one-dimensional traps.[31] A theoretical analysis of a BEC on an ellipsoidal waveguide can be seen in Refs. 26 and 32 and on any kind of one-dimensional geometry in Ref. 33.

Recently, the prospects of observing a Bose gas on a two-dimensional curved manifold became a reality with a type of

confinement known as a *bubble trap*.[34,35] This experiment was initially proposed in Refs. 36–38, involving atoms dressed by a radio frequency field trapped in an inhomogeneous magnetic field. With this, it is possible to let the gas be confined to the surface of an ellipsoidal shape. The first experimental realization of a Bose gas in the thermal state on the surface of an ellipsoid using this technique was performed in Ref. 39. Attempts to reach the BEC state were performed in the same experiment;[40–42] however, it happened that the gas was found only on the bottom of this bubble due to the gravitational sag. Thus, it became necessary to find alternative routes to implement this bubble shape successfully.

The first one of these routes was to launch this experiment to the International Spacial Station (ISS) of NASA, where a cold atom laboratory was developed to perform a variety of experiments with fermionic and bosonic cold gases.[43–46] A little time after the first realization of a BEC in ISS,[47] it was reported the first step on the bubble trap experiments: an ultra-cold Bose gas was confined on the surface of a bubble trap,[34] where the gas is found in thermal states. The second route to implement experimentally the bubble trap happened in a terrestrial laboratory using an alternative technique based on the use of dual atomic species,[35] a method proposed in Refs. 48–50. Realizing the cold gas in the BEC state on a bubble trap is still being a challenge in all these experiments, and in Refs. 51 and 52, one can find the perspectives for all these developments. Finally, further routes are also being explored to compensate gravity and will enable the implementation a bubble trap with the radio frequency dressing technique on the ground as well.[53]

Motivated by these experimental achievements, diverse topics concerning BECs on a bubble trap were explored theoretically. Collective modes were computed using diverse methods[54–59] which, in particular, can characterize the crossover from a full sphere to a hollowed one.[57,58] The critical temperature of a BEC on the surface of a sphere was computed in Refs. 60–62, and the superfluid transition was characterized in Ref. 63. The stability of the fluid phase was analyzed in Refs. 64 and 65 and of stationary states of a BEC in Refs. 66 and 67. The self-interference in a bubble trap in free expansion is studied in Refs. 56 and 68 and its thermodynamic properties in Ref. 62. The authors of Ref. 69 propose a scheme that enables the generation of a slowly expanding shell with an isotropic momentum distribution. Furthermore, dipolar gases are explored on the surface of a sphere in Refs. 59, 65, and 70–72 and vortice dynamics in Refs. 73–75, while atomic interaction properties are characterized in Refs. 76 and 77. A review of these topics can be seen in Refs. 52 and 78.

For simplicity, the majority of the theoretical analyses describe the bubble as a perfect sphere, even though an ellipsoidal shape would be a better approximation.[41] Nevertheless, a sphere is a good approximation, including the fact that the topological properties of these two geometrical shapes are the same.[63] Among a few works that describe the bubble trap as an ellipsoid,[78–80] in Ref. 68, the authors compute the ground state of a BEC confined on such a surface and find a higher atomic accumulation on the poles of a prolate ellipsoid. Additionally, the thermal Bose gas in the experimental realizations shows similar behavior.[34]

In the present manuscript, we also compute the ground state of a BEC on an ellipsoid. In particular, we show that the geometric properties of an ellipsoid lead to an opposite ground state profile as the one above described: they induce a higher accumulation of atoms on the equator of a prolate ellipsoid, and not on the poles. Here, we are going to derive these results and explain this difference.

We initially derive our results for any kind of curved surface, where we obtain a two-dimensional Gross–Pitaevskii (2DGP) equation and a Thomas–Fermi solution. Subsequently, we apply these equations to the specific case of an ellipsoid, allowing us to discuss applications on a bubble trap and make a comparison with the ground state profile from Refs. 34 and 68. We work with a perturbative method, inspired by tools from Ref. 81, followed by a dimensional reduction technique, where we integrate the variable perpendicular to the surface. We obtain the 2DGP equation, where a term can be interpreted as a low-dimensional effective potential and depends on the curvatures of the surface. This is a term known as the *geometric potential*,[2,3] and it is responsible for the accumulation of atoms on the equator of a prolate ellipsoid.

We proceed as follows: In Sec. II, we introduce the mathematical objects we are going to use, where many of these tools were already used in a previous manuscript from one of us.[54] In Sec. III, we establish the physical model we are going to work on: we define the hypotheses on the confinement frequency and the strength of the interactions. In Sec. IV, we develop the perturbative expansion, in Sec. V, we employ the dimensional reduction, and in Sec. VI, we explore the Thomas–Fermi solution, for any kind of surface. In Sec. VII, we define an ellipsoid inspired by the experimental parameters of a bubble trap, and in Sec. VIII, we compare our results with the literature. In Sec. IX, we present a discussion and in Sec. X our conclusions.

II. MATHEMATICAL PRELIMINARIES

In this section, we introduce the mathematical objects that are necessary for the development of the paper. We closely follow the methods of a previous work by one of us,[54] where the reader can find a similar introductory section. The content of this section can be found in textbooks[82–84] and other references, such as Refs. 85–87.

Let us consider a smooth surface $\mathscr{M}$, that is, a two-dimensional differentiable manifold embedded in the three-dimensional Euclidean space. Assume that a given portion of $\mathscr{M}$ can be described by the two variables x^1 and x^2. That is, any point $\mathbf{p}$ that belongs to this surface portion can be expressed as $\mathbf{p} = (x^1, x^2)$. Since $\mathscr{M}$ belongs to the 3D space, these two variables might be expressed as functions of the Cartesian coordinates (x, y, z). On a surface, it is possible to define curvatures in more than one way. Important definitions are the principal curvatures κ_1 and κ_2, the mean curvature H, and the Gaussian curvature K.

To define the principal curvatures, let us first define the curvature of a curve on a plane, that is, of a one-dimensional manifold embedded in the two-dimensional Euclidean space. A curve on a plane can be described by a parametrized equation of the type $\gamma(t) = (x(t), y(t))$, such that $\|\gamma'(t)\| = \sqrt{x'(t)^2 + y'(t)^2} = 1$. The tangent vector to this curve is given by $\gamma'(t)$, and its curvature is given by $\kappa(t) = \|\gamma''(t)\|$. The interpretation of this curvature is that it is the inverse of the radius of the circle that is the best approximation to the curve $\gamma(t)$ at the respective point.

Now, let us consider again the surface $\mathscr{M}$, a specific point $\mathbf{p}(x^1, x^2)$ on this surface and the normal vector $\mathbf{n}(\mathbf{p})$ to $\mathscr{M}$ at $\mathbf{p}$. There is an infinite set of planes with origin at $\mathbf{p}$ and parallel to $\mathbf{n}(\mathbf{p})$. Each of these planes intersects the manifold $\mathscr{M}$, and this intersection is a curve on a plane, as described in the previous paragraph. Take this infinite

set of curves and their respective curvatures at $\mathbf{p}$, and consider the maximum and minimum among these curvatures. This defines the principal curvatures $\kappa_1(x^1, x^2)$ and $\kappa_2(x^1, x^2)$.

The mean and Gaussian curvatures are defined as

$$H(x^1, x^2) = \frac{\kappa_1(x^1, x^2) + \kappa_2(x^1, x^2)}{2} \tag{1}$$

and

$$K(x^1, x^2) = \kappa_1(x^1, x^2)\kappa_2(x^1, x^2). \tag{2}$$

Conversely, one can also obtain that

$$\kappa_i(x^1, x^2) = H(x^1, x^2) \pm \sqrt{H^2(x^1, x^2) - K(x^1, x^2)}. \tag{3}$$

Remember that the mean curvature of a curve at a given point is the inverse of the radius of the circle that best fits on a curve at this point. For the surface $\mathscr{M}$, let us define

$$R(x^1, x^2) = \min\left\{\frac{1}{\kappa_1(x^1, x^2)}, \frac{1}{\kappa_2(x^1, x^2)}\right\}, \tag{4}$$

which is the radius of the smaller circle that fits on a path on the surface at $\mathbf{p} = (x^1, x^2)$, as we explained in the above paragraph. It is also possible to define the minimum among the radii $R(x^1, x^2)$

$$R = \min\{R(x^1, x^2), \text{ for } (x^1, x^2) \in \mathscr{M}\}. \tag{5}$$

For a compact surface, R is strictly positive.

Let us now consider the three-dimensional space in the vicinity of a portion of the smooth surface $\mathscr{M}$ that contains $\mathbf{p} = (x^1, x^2)$. Consider a point $\mathbf{q}$ in the vicinity of $\mathscr{M}$ and suppose that the distance $d\{\mathbf{q}, \mathscr{M}\}$ between $\mathbf{q}$ and $\mathscr{M}$ is given by the distance $d\{\mathbf{q}, \mathbf{p}\}$ between $\mathbf{q}$ and $\mathbf{p}$. That is, $\mathbf{p}$ is the point on $\mathscr{M}$ that is the closest to $\mathbf{q}$.

With this, we can introduce the Gaussian normal coordinate system that describes the three-dimensional space and is represented by the variables (x^0, x^1, x^2). The variable x^0 is defined as the distance from a given point to the manifold, and the variables (x^1, x^2) are defined as their values on the point on $\mathscr{M}$ that is the closest. That is, in the Gaussian normal coordinate system, the point $\mathbf{q}$ as described above is given by

$$\mathbf{q} = (x^0, x^1, x^2) = (d\{\mathbf{q}, \mathbf{p}\}, x^1, x^2), \tag{6}$$

while the point $\mathbf{p}$ that is on the surface is given by

$$\mathbf{p} = (0, x^1, x^2). \tag{7}$$

The Gaussian normal coordinate system is well-defined only in the vicinity of the manifold, where $|x^0| < R$. With this, each point is described by a unique combination of variables x^0, x^1, and x^2. For simplicity, we will consider $-R/2 < x^0 < R/2$. With this, we define the neighborhood $\mathscr{N}(\mathscr{M})$ of $\mathscr{M}$ as the points $\mathbf{q} = (x^0, x^1, x^2)$ of the 3D space described by the Gaussian normal coordinate system, with $|x^0| < R/2$.

The metric of a manifold is defined as a matrix whose entrances are the internal product between the tangent vectors

$$G_{\mu\nu} = \mathbf{v}_\mu \cdot \mathbf{v}_\nu, \tag{8}$$

where $\mathbf{v}_\mu = \partial\mathbf{q}/\partial x^\mu$, for $\mu = 0, 1, 2$. The metric of the three-dimensional space in the Gaussian normal coordinates in the vicinity of $\mathscr{M}$ is given by[54]

$$G_{\mu\nu}(x^0, x^1, x^2) = \begin{pmatrix} 1 & 0 & 0 \\ 0 & & \\ 0 & & g_{ij}(x^0, x^1, x^2) \end{pmatrix}, \tag{9}$$

and the metric of the surface $\mathscr{M}$ is given by

$$(g_0)_{ij}(x^1, x^2) = g_{ij}(0, x^1, x^2). \tag{10}$$

From Appendix A of Ref. 54, one can see the relation of the metric in the Gaussian normal coordinate system and the above curvatures

$$\begin{aligned} \det g(x^0) = \det g_0 \big[1 + 4x^0 H + (x^0)^2(4H^2 + 2K) \\ + 4(x^0)^3 HK + (x^0)^4 K^2\big], \end{aligned} \tag{11}$$

where we hide the dependence of g, g_0, H, and K on x^1 and x^2 for brevity. Note that this is an exact formula. Moreover, this metric determinant can be re-expressed with the principal curvatures as

$$\det g(x^0) = \det g_0 (1 + \kappa_1 x^0)^2 (1 + \kappa_2 x^0)^2. \tag{12}$$

The Laplacian in Gaussian normal coordinates can be written as

$$\Delta = \frac{\partial^2}{\partial x^{02}} + \frac{\partial}{\partial x^0}\left(\ln\sqrt{\det g(x^0)}\right)\frac{\partial}{\partial x^0} + \Delta_{\mathscr{M}(x^0)}, \tag{13}$$

with the abbreviation

$$\Delta_{\mathscr{M}(x^0)} = \frac{1}{\sqrt{\det g(x^0)}}\frac{\partial}{\partial x^i}\left(\sqrt{\det g(x^0)}\, g^{ij}(x^0)\frac{\partial}{\partial x^j}\right). \tag{14}$$

All the mathematical objects reviewed here are going to be used within a physical model to derive our results.

III. MODEL

To study a Bose gas that is confined on a curved surface we must initially establish how it is confined there. For that, we are going to consider a modified harmonic trap as the following. Significantly, this confinement must be strong, so that the gas behavior becomes almost two-dimensional.

To that, let us choose a harmonic frequency ω_0, with the condition that the corresponding one-dimensional cloud width $\sigma_0 = \sqrt{\hbar/m\omega_0}$ satisfies $\sigma_0/R \ll 1$. Here, $\hbar$ is the Planck constant and m is the mass of the confined particles.

We consider then the following confinement potential:

$$\begin{aligned} U_{\text{trap}}(x^0, x^1, x^2) &= \frac{m\left[\omega_0 + \omega_2(x^1, x^2)\right]^2}{2}(x^0)^2 \\ &= \frac{m\omega_0^2}{2}(x^0)^2 + m\omega_0\omega_2(x^1, x^2)(x^0)^2 \\ &\quad + \frac{m\omega_2(x^1, x^2)^2}{2}(x^0)^2. \end{aligned} \tag{15}$$

By definition, we have that

$$\mathscr{O}\left(\frac{\omega_0}{\omega_R}\right) = \mathscr{O}\left(\left[\frac{\sigma_0}{R}\right]^{-2}\right), \tag{16}$$

where we introduced $\omega_R = \hbar/mR^2$ for a dimensionless comparison of orders of magnitude. Importantly, we impose that

$$\mathcal{O}\left(\frac{\omega_2(x^1,x^2)}{\omega_R}\right)=\mathcal{O}(1), \tag{17}$$

for all x^1 and x^2 where the Gaussian normal coordinate system is well-defined.

Note that, for completeness, we could have added a term $m\omega_1(x^0)^2/2$, with $\mathcal{O}(\omega_1/\omega_R)=\mathcal{O}((\sigma_0/R)^{-1})$ in the above potential. However, we would have imposed it to be constant as well, thus it can be absorbed into the factor ω_0 without any loss of generality. The reason we impose these frequencies to be constants is that, without these constraints, it is not possible to perform a dimensional reduction for any infinitely thin manifold. In general, divergent terms would appear in the limit $\sigma_0\to 0$, and the gas would accumulate at a specific point rather than being distributed across the surface. A well-defined dimensional reduction was performed for a case where ω_0 is not constant in Ref. 55, where the studied surface is asymptotically a sphere.

The wave function $\Psi(x^0,x^1,x^2)$ that is a solution or an approximate solution for the ground state of a gas confined in the potential (15) for $\sigma_0\ll R$ is expected to be concentrated in the neighborhood of the surface $\mathscr{M}$. That is, we expect that a good approximation for the particle number is given by

$$N\simeq\int_{-R/2}^{R/2}dx^0\int dx^1dx^2\sqrt{g(x^0,x^1,x^2)}\|\Psi(x^0,x^1,x^2)\|^2. \tag{18}$$

Moreover, any other quantity related to the wave function can also be computed considering only this spatial region.

Finally, we consider that the interaction strength g_{int} among the atoms is weak. Specifically, we consider that

$$\mathcal{O}\left(\frac{a_s}{R}\right)=\mathcal{O}\left(\frac{\sigma_0}{R}\right), \tag{19}$$

where a_s is the scattering length with the relation $g_{\text{int}}=4\pi\hbar^2a_s/M$. This hypothesis is not strictly necessary to study a dimensional reduction. For instance, in Refs. 57,58, they studied the behavior of a quasi-two-dimensional sphere considering strong interactions. Here, we make this choice of such weak interactions in order to study the influence of interactions just after performing a dimensional reduction.

IV. PERTURBATIVE EXPANSION

In this section, we develop part of our methodical calculations. Readers who prefer to skip the technical details may read only the next paragraph, where we summarize the main steps of this section, and the last two paragraphs, where we motivate the calculations of Sec. V.

Here, we consider a general Ansatz for the wave function given by Eq. (23), with the conditions (24) and (25). We insert this Ansatz into the GP equation, which is given by expression (20), in a short form, and by expression (22), in an extended form. We follow a perturbative expansion in orders $\mathcal{O}(\sigma_0/R)$. The first order to be considered is $\mathcal{O}([\sigma_0/R]^{-2})$, from which we obtain the solution for the term e^{S_0} from the Ansatz (23), which is proportional to the Gaussian wave function $\mathcal{G}$ from Eq. (32). This term guarantees that the wave function is exponentially small far from the surface $\mathscr{M}$. We proceed to the next order $\mathcal{O}([\sigma_0/R]^{-1})$. From this step, we obtain a partial solution for the term e^{S_1} from the Ansatz (23), which is given in Eq. (39). From these findings, we can express the Ansatz as in Eq. (41), where ψ must satisfy Eq. (43) up to order $\mathcal{O}(1)$. Equation (43) thus is the development of the GP equation (20) with the imposed Ansatz.

With (41) and (43), it is possible to proceed to Sec. V. In the following, we perform the above-described systematic calculations.

We intend to solve approximately the Gross–Pitaevskii (GP) equation

$$-\mu\Psi-\frac{\hbar^2}{2m}\Delta\Psi+U_{\text{trap}}+g_{\text{int}}|\Psi|^2\Psi=0, \tag{20}$$

which can be denoted as

$$\text{GP}(\Psi)=0. \tag{21}$$

Inserting the potential (15) and the expression (13) for the Laplacian into the above equation, the GP equation in Gaussian normal coordinates becomes

$$\begin{aligned}&-\mu\Psi-\frac{\hbar^2}{2m}\left(\frac{\partial^2}{\partial(x^0)^2}+\left[\frac{\partial\ln\sqrt{\det g}}{\partial x^0}\right]\frac{\partial}{\partial x^0}+\Delta_{\mathscr{M}(x^0)}\right)\Psi\\&+\frac{m\omega_0^2}{2}(x^0)^2\Psi+m\omega_0\omega_2(x^0)^2\Psi+\frac{m\omega_2^2}{2}(x^0)^2\Psi\\&+g_{\text{int}}|\Psi|^2\Psi=0.\end{aligned} \tag{22}$$

To solve approximately this equation, we are going to consider the following Ansatz:

$$\Psi(x^0,x^1,x^2)=\alpha^{1/2}e^{S_0(x^0,x^1,x^2)+S_1(x^0,x^1,x^2)+\cdots}, \tag{23}$$

where α is a constant defined by the units chosen to describe the problem. Importantly, close to the surface $\mathscr{M}$, specifically, where $\mathcal{O}(x^0/R)=\mathcal{O}(\sigma_0/R)$, we assume the following:

$$\mathcal{O}\left(R\frac{\partial S_0}{\partial x^0}\right)=\mathcal{O}\left(\left[\frac{\sigma_0}{R}\right]^{-1}\right),\quad \mathcal{O}\left(R^2\frac{\partial^2S_0}{\partial(x^0)^2}\right)=\mathcal{O}\left(\left[\frac{\sigma_0}{R}\right]^{-2}\right); \tag{24}$$

$$\mathcal{O}\left(R\frac{\partial S_1}{\partial x^0}\right)=\mathcal{O}\left(R^2\frac{\partial^2S_1}{\partial(x^0)^2}\right)=\mathcal{O}(1). \tag{25}$$

The above hypotheses (24) and (25) are motivated by assumptions (16) and (17), and inspired by the approach developed in Ref. 81. Note that S_0 represents the term responsible for Ψ being very sharp in the vicinity of the surface $\mathscr{M}$.

Generally, we also consider that $\mathcal{O}(R\partial S_n/\partial x^0)=\mathcal{O}([\sigma_0/R]^{n-1})$ and $\mathcal{O}(R^2\partial^2S_n/\partial(x^0)^2)=\mathcal{O}([\sigma_0/R]^{n-2})$, for $x^0\simeq\sigma_0$ and $n\geq 2$. However, we will need only terms until order $\mathcal{O}(1)$ to reach our results, meaning that we will neglect terms of orders $\mathcal{O}(\sigma_0/R)$ or higher. With this only the terms S_0 and S_1 are relevant to our calculations. The terms associated with S_2 vanish under the approximations we are making, and we show it in Appendix C. To be precise, we would need to include the terms associated with S_2 in the following calculations, but for simplicity, we will already now ignore them. Moreover, the terms associated with S_n, for $n\geq 3$ are of order $\mathcal{O}(\sigma_0/R)$ or higher, and we already neglect them now.

Evaluating the first and second derivatives of Ψ, we obtain

$$\begin{aligned}\frac{\partial\Psi}{\partial x^0}&=(S_0'+S_1')\Psi\ \text{ and}\\\frac{\partial^2\Psi}{\partial(x^0)^2}&=(S_0''+S_0'^2+2S_0'S_1'+S_1''+S_1'^2)\Psi.\end{aligned} \tag{26}$$

Inserting these expressions with the above Ansatz into the GP equation and dividing it by Ψ, we obtain approximately that

$$-(\mu_0+\mu_1+\mu_2)-\frac{\hbar^2}{2m}\left(S_0''+S_0'^2+2S_0'S_1'+S_1''+S_1'^2+\left[\frac{\partial \ln\sqrt{\det g}}{\partial x^0}\right](S_0'+S_1')\right)-\frac{\hbar^2}{2m}\frac{\Delta_{\mathscr{M}(x^0)}\Psi}{\Psi}+\frac{m\omega_0^2}{2}(x^0)^2+m\omega_0\omega_2(x^0)^2+\frac{m\omega_2^2}{2}(x^0)^2+g_{\text{int}}|\Psi|^2=0. \tag{27}$$

where we divided the chemical potential into three terms of orders

$$\mathscr{O}\left(\frac{\mu_0}{\mu_R}\right)=\mathscr{O}\left(\left[\frac{\sigma_0}{R}\right]^{-2}\right),\quad \mathscr{O}\left(\frac{\mu_1}{\mu_R}\right)=\mathscr{O}\left(\left[\frac{\sigma_0}{R}\right]^{-1}\right),\quad \mathscr{O}\left(\frac{\mu_2}{\mu_R}\right)=\mathscr{O}(1), \tag{28}$$

where $\mu_R=\hbar\omega_R/2$ is introduced for a dimensionless comparison.

Notably, the above equation is valid only for the range where

$$\mathscr{O}\left(\frac{x^0}{R}\right)=\mathscr{O}\left(\frac{\sigma_0}{R}\right). \tag{29}$$

This constraint occurs because we already have that $\Psi\simeq 0$ outside this range, and consequently, the GP equation (22) is approximately satisfied automatically. Therefore, we can only impose equation (27) to be approximately valid in the range (29).

Now, considering only the terms of order $\mathscr{O}([\sigma_0/R]^{-2})$ in Eq. (27), we obtain

$$-\mu_0-\frac{\hbar^2}{2m}(S_0''+S_0'^2)+\frac{m\omega_0^2}{2}(x^0)^2=0, \tag{30}$$

where we remind that $\mathscr{O}(\omega_0^2/\omega_R^2)=\mathscr{O}([\sigma_0/R]^{-4})$ and $\mathscr{O}([x^0]^2/R^2)=\mathscr{O}(\sigma_0^2/R^2)$, leading to $\mathscr{O}(\omega_0^2[x^0]^2/[\omega_R^2R^2])=\mathscr{O}([\sigma_0/R]^{-2})$.

Denoting $\mathscr{G}=\pi^{-1/4}\sigma_0^{-1/2}e^{S_0}$, we have that $\mathscr{G}''=(S_0''+S_0'^2)\mathscr{G}$ and the above equation is simply the equilibrium equation of a one-dimensional quantum harmonic oscillator

$$-\mu_0\mathscr{G}-\frac{\hbar^2}{2m}\mathscr{G}''+\frac{m\omega_0^2}{2}(x^0)^2\mathscr{G}=0, \tag{31}$$

leading to the following Gaussian wave-function and chemical potential

$$\mathscr{G}(x^0)=\frac{e^{-(x^0)^2/2\sigma_0^2}}{\sqrt[4]{\pi}\sqrt{\sigma_0}},\quad \mu_0=\frac{\hbar\omega_0}{2}. \tag{32}$$

Consequently, we obtain that

$$S_0(x^0)=-\frac{(x^0)^2}{2\sigma_0^2},\quad S_0'(x^0)=-\frac{x^0}{\sigma_0^2},\quad S_0''(x^0)=-\frac{1}{\sigma_0^2}. \tag{33}$$

Note that this solution is consistent with hypotheses (24) and that S_0 is independent on the variables x^1 and x^2. With this, the ansatz (23) can be rewritten as

$$\Psi(x^0,x^1,x^2)=\mathscr{G}(x^0)\psi(x^0,x^1,x^2), \tag{34}$$

where $\psi(x^0,x^1,x^2)=\pi^{1/4}\sigma_0^{1/2}\alpha^{1/2}e^{S_1(x^0,x^1,x^2)}$. Remember that here we are already ignoring the terms S_n, for $n\geq 2$.

With expression (34), GP equation (27) becomes

$$-(\mu_1+\mu_2)-\frac{\hbar^2}{2m}\left(2S_0'S_1'+S_1''+S_1'^2+\left[\frac{\partial\ln\sqrt{\det g}}{\partial x^0}\right](S_0'+S_1')\right)-\frac{\hbar^2}{2m}\frac{\Delta_{\mathscr{M}(x^0)}\psi}{\psi}+m\omega_0\omega_2(x^0)^2+\frac{m\omega_2^2}{2}(x^0)^2+g_{\text{int}}\mathscr{G}^2|\psi|^2=0, \tag{35}$$

which is also valid only in regime (29). Now, considering only the terms of order $\mathscr{O}([\sigma_0/R]^{-1})$, the above equation becomes

$$-\mu_1+\frac{\hbar^2x^0}{m\sigma_0^2}\left(S_1'+\frac{1}{2}\left[\frac{\partial\ln\sqrt{\det g}}{\partial x^0}\right]\right)=0, \tag{36}$$

which imposes that $\mu_1=0$ (see Appendix A) and that

$$\frac{\partial S_1}{\partial x^0}=\frac{\partial\ln\left((\det g)^{-1/4}\right)}{\partial x^0}. \tag{37}$$

Integrating this equation on x^0, we obtain

$$S_1(x^0,x^1,x^2)=\ln\left(\left[\det g(x^0,x^1,x^2)\right]^{-1/4}\right)+\overline{S_1}(x^1,x^2), \tag{38}$$

and then

$$e^{S_1(x^0,x^1,x^2)}=\frac{e^{\overline{S}_1(x^1,x^2)}}{\sqrt[4]{\det g(x^0,x^1,x^2)}}. \tag{39}$$

Denote $\phi(x^1,x^2)=\pi^{1/4}(\alpha\sigma_0)^{1/2}e^{\overline{S}_1(x^1,x^2)}/\sqrt[4]{\det g_0(x^1,x^2)}$. Considering expression (32), Ansatz (23) takes the form

$$\Psi(x^0,x^1,x^2)=\mathscr{G}(x^0)\frac{\sqrt[4]{\det g_0(x^1,x^2)}}{\sqrt[4]{\det g(x^0,x^1,x^2)}}\phi(x^1,x^2), \tag{40}$$

which is the same Ansatz as the proposed one in Ref. 54, but written in a slightly different way. There, the term $\sqrt[4]{\det g(x^0,x^1,x^2)}$ was introduced to maintain the error in the calculation of the particle number exponentially small. Without this term, this error would have a quadratic decrease within the ratio σ_0/R. In the present paper, we derived this Ansatz from more general hypotheses and more elementary methods. Moreover, the dimensional reduction in Ref. 54 was treated in a quasi-two-dimensional limit so that the dependence of σ_0 on the variables x^1 and x^2 was considered. In the present paper, we consider σ_0 as a constant.

From Eq. (12), Ansatz (40) can be rewritten as

$$\Psi(x^0,x^1,x^2)=\mathscr{G}(x^0)\psi(x^0,x^1,x^2)=\frac{\mathscr{G}(x^0)\phi(x^1,x^2)}{\sqrt{(1+\kappa_1x^0)(1+\kappa_2x^0)}}. \tag{41}$$

Remember that this solution is written in Gaussian normal coordinate systems, which is well-defined only for $|x^0|<R$, where $R=\min\{1/\kappa_1,1/\kappa_2\}$. Consequently, the term $\sqrt{(1+\kappa_1x^0)(1+\kappa_2x^0)}$ never vanishes.

Turning back our attention to the GP equation, from solution (37), we obtain that expression (35) becomes

$$-\mu_2\mathcal{G}\psi-\frac{\hbar^2}{2m}\left(-\frac{1}{2}\left[\frac{\partial^2\ln\sqrt{\det g}}{\partial(x^0)^2}\right]-\frac{1}{4}\left[\frac{\partial\ln\sqrt{\det g}}{\partial x^0}\right]^2\right)\mathcal{G}\psi$$
$$-\frac{\hbar^2}{2m}(\Delta_{\mathcal{M}(x^0)}\psi)\mathcal{G}+m\omega_0\omega_2(x^0)^2\mathcal{G}\psi+\frac{m\omega_2^2}{2}(x^0)^2\mathcal{G}\psi$$
$$+g_{\rm int}\mathcal{G}^3|\psi|^2\psi=0. \tag{42}$$

Here, note that Ψ does not appear in the denominator anymore. Thus, the above equation is valid for all x^0 where the Gaussian normal coordinate system is well defined, that is, for $-R/2<x^0<R/2$.

Moreover, observe that Eqs. (30) and (36) exactly vanish. This can be verified by checking these equations with Ansatz (34).

Reminding that $m\omega_0=\hbar/\sigma_0^2$ and using Eq. (12), the above expression (42) takes the form

$$-\mu_2\mathcal{G}\psi-\frac{\hbar^2}{8m}\left(\frac{\kappa_1}{1+\kappa_1x^0}-\frac{\kappa_2}{1+\kappa_2x^0}\right)^2\mathcal{G}\psi-\frac{\hbar^2}{2m}(\Delta_{\mathcal{M}(x^0)}\psi)\mathcal{G}$$
$$+\frac{\hbar\omega_2}{\sigma_0^2}(x^0)^2\mathcal{G}\psi+\frac{m\omega_2^2}{2}(x^0)^2\mathcal{G}\psi+g_{\rm int}\mathcal{G}^3|\psi|^2\psi=0. \tag{43}$$

To further evaluate this expression, we would need to compute higher orders of the ansatz Ψ, taking into account the terms S_2, S_3, and so on. However, we decided to only consider terms until order $\mathcal{O}(1)$. Thus, we can neglect S_n, for $n\geq 2$, and need to find an approximate solution for $\psi(x^0,x^1,x^2)$. To do that, remember that we assume $\sigma_0\ll R$, meaning that the function $\mathcal{G}(x^0)$ is extremely sharp. This means that the value of $\psi(x^0,x^1,x^2)$ is relevant only for small values of x^0, which is where $\psi(x^0,x^1,x^2)\simeq\phi(x^1,x^2)$. Motivated by this reasoning, we will make a dimensional reduction, which allows us to define a two-dimensional Gross–Pitaevski (2DGP) equation for the two-dimensional wave function $\phi(x^1,x^2)$.

A second reason for choosing to perform a dimensional reduction is that, differently from the previous steps, where we computed the terms of orders $\mathcal{O}([\sigma_0/R]^{-2})$ and $\mathcal{O}([\sigma_0/R]^{-1})$, we now have to consider the nonlinear term $g_{\rm int}\mathcal{G}^3|\psi|^2\psi$. In the previous steps, we factorized the term $\mathcal{G}(x^0)$ and played with polynomials, where we could clearly identify the orders of magnitude in σ_0/R for all terms, considering that $\mathcal{O}(x^0/R)=\mathcal{O}(\sigma_0/R)$. Now, it is not clear how to evaluate the orders of magnitude with the functions $\mathcal{G}(x^0)$ and $\mathcal{G}^3(x^0)$, since we cannot factorize these terms anymore. With the dimensional reduction method, we will recover the transparency on the orders of magnitude.

V. DIMENSIONAL REDUCTION

In Sec. IV, we derived an approximate Anzats for the wave function of a gas on a surface $\mathcal{M}$ with the confinement potential given in (15)–(17). The wave function is given in expression (41), where the Gaussian wave function $\mathcal{G}$ is found in expression (32), and the term $\psi(x^0,x^1,x^2)=\phi(x^1,x^2)/\sqrt{(1+\kappa_1x^0)(1+\kappa_2x^0)}$ must satisfy Eq. (43) up to order $\mathcal{O}(1)$. In this section, we are going to perform a dimensional reduction on Eq. (43), leading to a 2DGP equation that is satisfied by the two-dimensional wave function $\phi(x^1,x^2)$.

In this procedure, we multiply Eq. (43) by the function $\sqrt{(1+\kappa_1x^0)(1+\kappa_2x^0)}\,\mathcal{G}$ and integrate it only with respect to the x^0 variable on the limit $\sigma_0\to 0$. The reasons for the multiplicative terms are computational convenience and for guaranteeing well-defined integrals in the limit of a thin shell, which are thoroughly explained in the following. Readers who prefer to skip the technical details of this section may consider simply Eqs. (46) and (53)–(55).

To derive the dimensional reduction of Eq. (43), observe that its left side vanishes up to order $\mathcal{O}(1)$. We can multiply this equation by any function that admits a Taylor expansion of the type $1+\sum_n a_n(x^0)^n$, with $\mathcal{O}(a_n)=\mathcal{O}(R^{-n})$, without altering its leading-order terms. Note that the expression $\sqrt{(1+\kappa_1x^0)(1+\kappa_2x^0)}$ features exactly this kind of Taylor expansion. Therefore, for computational convenience, we multiply Eq. (43) by this expression.

Moreover, it is expected that the integral of the left side of (43) would vanish, since the integral of zero should remain zero. However, this is a subtle process in the limit of a thin shell, where $\omega_0\to\infty$ and $\sigma_0\to 0$. The Gaussian distribution, which is the square of the Gaussian wave function, is a well-defined function for finite σ_0 and it tends to the Dirac delta distribution in the thin shell limit: $\lim_{\sigma_0\to0}\mathcal{G}^2(x^0)=\delta(x^0)$. According to the theory of distributions,[88] the Dirac delta $\delta(x^0)$ is a well-defined mathematical object. The limit of the following integral can be computed as:

$$\lim_{\sigma_0\to0}\int_{\mathcal{N}\{x^0=0\}}f(x^0)\mathcal{G}^2(x^0)dx^0=\int_{\mathcal{N}\{x^0=0\}}f(x^0)\delta(x^0)dx^0=f(0), \tag{44}$$

where the integral is performed on any neighborhood $\mathcal{N}\{x^0=0\}$ around $x^0=0$ and $f(x^0)$ is any well-behaved function on this neighborhood. For simplicity, let us consider that this neighborhood is given by the interval $[-R/2,R/2]$, in which we can guarantee that the Gaussian normal coordinate system is well defined.

However, note that the limit $\lim_{\sigma_0\to0}\mathcal{G}(x^0)$ is not a well-defined mathematical object. As a result, simply integrating the left side of Eq. (43) with respect to x^0 in the limit of a thin shell would not constitute a valid mathematical operation. To perform a proper integration, we must multiply Eq. (43) by $\mathcal{G}$, and afterwards integrate it with respect to x^0.

This argument can be applied directly to nearly all the terms of Eq. (43), including the term $(\hbar\omega_2/\sigma_0^2)(x^0)^2\mathcal{G}\psi$, even with the dependence of its quotient $(x^0)^2/\sigma_0^2$ on σ_0. Although this may not be immediately evident, the limit below is a well-defined distribution

$$\lim_{\sigma_0\to0}\frac{(x^0)^2}{\sigma_0^2}\mathcal{G}^2(x^0)=\frac{\delta(x^0)}{2} \tag{45}$$

as one can check in Appendix B.

The non-linear term $g_{\rm int}\mathcal{G}^3|\psi|^2\psi$ is the only one we cannot directly integrate with respect to x^0. Multiplying it by $\mathcal{G}$, we obtain the function $\mathcal{G}^4$, which is not a well-defined distribution in the limit of a thin shell. To be able to deal with this term using the method above described, we proceed as the following. Rather than treating $g_{\rm int}$ as a finite valued constant, we treat it as a function of σ_0 with the condition that $\lim_{\sigma_0\to0}g_{\rm int}=0$. Therefore, let us assume that

$$g_{\rm int}=\sqrt{2\pi}g_{\rm 2D}\,\sigma_0, \tag{46}$$

where $g_{\rm 2D}$ is a constant that we refer to as *two-dimensional interaction strength*. We can conclude that

$$g_{\rm int}\mathcal{G}^4=g_{\rm 2D}\frac{e^{\frac{(x^0)^2}{(\sigma_0/\sqrt{2})^2}}}{\sqrt{\pi}(\sigma_0/\sqrt{2})}, \tag{47}$$

which corresponds to the constant g_{2D} times a Gaussian distribution with standard deviation $\sigma_0/\sqrt{2}$. With this, the limit below becomes well-defined

$$\lim_{\sigma_0\to 0} g_{\rm int}\mathcal{G}^4 = g_{2D}\delta(x^0). \tag{48}$$

Now, let us follow the dimensional reduction method integrating Eq. (43) times $\sqrt{(1+\kappa_1 x^0)(1+\kappa_2 x^0)}\,\mathcal{G}(x^0)$ with respect to the variable x^0 in the limit of a thin shell

$$\lim_{\sigma_0\to 0}\int_{-R/2}^{R/2} dx^0\sqrt{(1+\kappa_1 x^0)(1+\kappa_2 x^0)}\,\mathcal{G}(x^0) \cdot {\rm GP}\big(\Psi(x^0,x^1,x^2)\big) = 0. \tag{49}$$

Evaluating the term ${\rm GP}(\Psi(x^0,x^1,x^2))$ according to Eq. (43), the above expression becomes

$$\begin{aligned}\lim_{\sigma_0\to 0}\int_{-R/2}^{R/2} dx^0\cdot\Bigg\{&-\mu_2\mathcal{G}^2\phi-\frac{\hbar^2}{8m}\left(\frac{\kappa_1}{1+\kappa_1 x^0}-\frac{\kappa_2}{1+\kappa_2 x^0}\right)^2\mathcal{G}^2\phi\\&-\frac{\hbar^2}{2m}(\Delta_{\mathcal{M}(x^0)}\phi)\mathcal{G}^2-\frac{\hbar^2}{2m}\sqrt{(1+\kappa_1 x^0)(1+\kappa_2 x^0)}\\&\left(\Delta_{\mathcal{M}(x^0)}\left[(1+\kappa_1 x^0)(1+\kappa_2 x^0)\right]^{-1/2}\right)\mathcal{G}^2\phi\\&-\frac{\hbar^2}{m}\sqrt{(1+\kappa_1 x^0)(1+\kappa_2 x^0)}g^{ij}\\&\left(\partial_i\left[(1+\kappa_1 x^0)(1+\kappa_2 x^0)\right]^{-1/2}\right)\mathcal{G}^2(\partial_j\phi)\\&+\frac{\hbar\omega_2}{\sigma_0^2}(x^0)^2\mathcal{G}^2\phi+\frac{m\omega_2^2}{2}(x^0)^2\mathcal{G}^2\phi\\&+\frac{g_{\rm int}\mathcal{G}^4|\phi|^2\phi}{(1+\kappa_1 x^0)(1+\kappa_2 x^0)}\Bigg\}=0,\end{aligned} \tag{50}$$

where we hide the dependence of $\mathcal{G}$ on x^0 and of ϕ, κ_1 and κ_2 on x^1, x^2 for simplicity.

Interchanging the limit $\lim_{\sigma_0\to 0}$ with the integral as it is done in Eq. (44), and considering Eqs. (45) and (48), the above expression becomes

$$\begin{aligned}\int_{-R/2}^{R/2} dx^0\Bigg\{&-\mu_2\phi-\frac{\hbar^2}{8m}\left(\frac{\kappa_1}{1+\kappa_1 x^0}-\frac{\kappa_2}{1+\kappa_2 x^0}\right)^2\phi\\&-\frac{\hbar^2}{2m}(\Delta_{\mathcal{M}(x^0)}\phi)-\frac{\hbar^2}{2m}\sqrt{(1+\kappa_1 x^0)(1+\kappa_2 x^0)}\\&\left(\Delta_{\mathcal{M}(x^0)}\left[(1+\kappa_1 x^0)(1+\kappa_2 x^0)\right]^{-1/4}\right)\phi\\&-\frac{\hbar^2}{m}\sqrt{(1+\kappa_1 x^0)(1+\kappa_2 x^0)}g^{ij}\\&\left(\partial_i\left[(1+\kappa_1 x^0)(1+\kappa_2 x^0)\right]^{-1/2}\right)(\partial_j\phi)\\&+\frac{\hbar\omega_2}{2}\phi+\frac{m\omega_2^2}{2}(x^0)^2\phi+\frac{g_{2D}|\phi|^2\phi}{(1+\kappa_1 x^0)(1+\kappa_2 x^0)}\Bigg\}\delta(x^0)=0.\end{aligned} \tag{51}$$

To perform this integral, we can attribute $x^0=0$ to all the terms inside the curly brackets. The only terms where this procedure requires more caution are those from second and third rows, because we need to perform the derivatives before replacing the value of x^0. One can check that the contribution of this term vanishes, being enough to verify that the derivatives ∂_i and $\partial_i\partial_j$ of the term $[(1+\kappa_1 x^0)\times(1+\kappa_2 x^0)]^{-1/4}$ vanish for $x^0=0$.

With this, the above integral becomes

$$-\mu_2\phi-\frac{\hbar^2}{8m}(\kappa_1-\kappa_2)^2\phi-\frac{\hbar^2}{2m}\Delta_{\mathcal{M}}\phi+\frac{\hbar\omega_2}{2}\phi+g_{2D}|\phi|^2\phi=0. \tag{52}$$

Denoting

$$V_{\rm geom}(x^1,x^2)=-\frac{\hbar^2}{8m}\left[\kappa_1(x^1,x^2)-\kappa_2(x^1,x^2)\right]^2 \tag{53}$$

as the geometric potential and

$$V_{\rm ext}(x^1,x^2)=\frac{\hbar\omega_2(x^1,x^2)}{2} \tag{54}$$

as the external potential, we can rewrite Eq. (52) as

$$\left(-\mu_2-\frac{\hbar^2}{2m}\Delta_{\mathcal{M}}+V_{\rm geom}+V_{\rm ext}+g_{2D}|\phi|^2\right)\phi=0, \tag{55}$$

where $\phi=\phi(x^1,x^2)$.

This is a 2DGP equation for the two-dimensional wave-function $\phi(x^1,x^2)$, where we obtain two effective potentials $V_{\rm geom}(x^1,x^2)$ and $V_{\rm ext}(x^1,x^2)$. The first potential depends on the curvatures $\kappa_1(x^1,x^2)$ and $\kappa_2(x^1,x^2)$ of the surface $\mathcal{M}$, while the latter can be any function, and it depends on the asymmetries of the second term of the confinement frequency $\omega_2(x^1,x^2)$.

The geometric potential $V_{\rm geom}$ was first developed in the seminal references.[2,3] In a previous Ref. 54 of some of us, we also computed this geometric potential, expressed in terms of the determinant of the metric g_0. Moreover, we did not explore further consequences of this term in that article, since we focused on applying our methods to a sphere, where the geometric potential vanishes. This happens because the principal curvatures κ_1 and κ_2 are equivalent on a sphere.

In Secs. VII and VIII, we are going to apply the 2DGP equation to an ellipsoid and compare the effects generated by the geometric and external potentials on the ground state.

VI. VI. THOMAS–FERMI APPROXIMATION

In the three-dimensional GP equation, the Thomas–Fermi approximation must be taken when the interactions $g_{\rm int}$ are strong. However, we assume that $g_{\rm int}$ are weak. In fact, according to Eq. (46), we have that $g_{\rm int}\to 0$ in the limit of a thin shell. Thus, within the model, we are working on, we cannot use Thomas–Fermi methods to solve Eq. (20).

On another side, in the 2DGP equation (55), the two-dimensional interactions are assumed to be the constant value g_{2D}. Considering this constant to be strong, we can apply the Thomas–Fermi solution to the 2DGP equation, and the ground state density is well-approximated by

$$|\phi_0(x^1,x^2)|^2=\frac{1}{g_{2D}}\left(\mu_2-\frac{\hbar\omega_2(x^1,x^2)}{2}+\frac{\hbar^2}{8m}\left[\kappa_1(x^1,x^2)-\kappa_2(x^1,x^2)\right]^2\right). \tag{56}$$

If ω_2 is a constant, then the ground state is fully defined by the difference between the mean curvatures. The higher density happens in the regions of the highest difference of curvatures κ_1 and κ_2.

With this, one can conclude that, in the absence of external asymmetries, geometric properties of the surface $\mathscr{M}$ can be directly observed by measuring the ground state of a Bose-gas confined in this area.

In Secs. VII and VIII, we will analyze the situation where the surface $\mathscr{M}$ is an ellipsoid, which is motivated by the bubble trap experiments.

VII. ELLIPSOID

Motivated by the current experiments to implement a bubble trap, we will apply the above formalism for a BEC confined on the surface of a prolate ellipsoid given by the following equation:

$$\frac{x^2}{a^2}+\frac{y^2}{a^2}+\frac{z^2}{b^2}=R^2, \tag{57}$$

in Cartesian coordinates, where a and b are dimensionless.

To study the ground state, we need to express the ellipsoid in two variables x^1 and x^2. To do that, we first consider the prolate spheroidal coordinates (r,φ,θ) to describe the three-dimensional space. It is given by the transformation

$$\begin{aligned} x &= ra\cos\theta\sin\varphi,\\ y &= ra\sin\theta\sin\varphi,\\ z &= rb\cos\varphi, \end{aligned} \tag{58}$$

where $r>0$, $\varphi\in[0,\pi]$, and $\theta\in[0,2\pi)$. A constant value of $r=R$ defines the ellipsoid of Eq. (57). Thus, we can describe the ellipsoid with the two variables $x^1=\varphi$ and $x^2=\theta$.

The mean and Gaussian curvatures for such an ellipsoid are given by

$$H=\frac{b}{2a}\frac{2a^2+(b^2-a^2)\sin^2\varphi}{(a^2\cos^2\varphi+b^2\sin^2\varphi)^{3/2}} \tag{59}$$

and

$$K=\frac{b^2}{(a^2\cos^2\varphi+b^2\sin^2\varphi)^2}. \tag{60}$$

Using relation (3), we obtain that $(\kappa_1-\kappa_2)^2=H^2-K$, and from the above formulas, the geometric potential is given by

$$V_{\text{geom}}=-\frac{\hbar^2}{8mR^2}\frac{b^2(a^2-b^2)^2\sin^4\varphi}{a^2\left[a^2\cos^2\varphi+b^2\sin^2\varphi\right]^3}. \tag{61}$$

Note that there is no dependence on θ, which is expected due to the symmetry of the ellipsoid. In Fig. 1, we plot the dependence

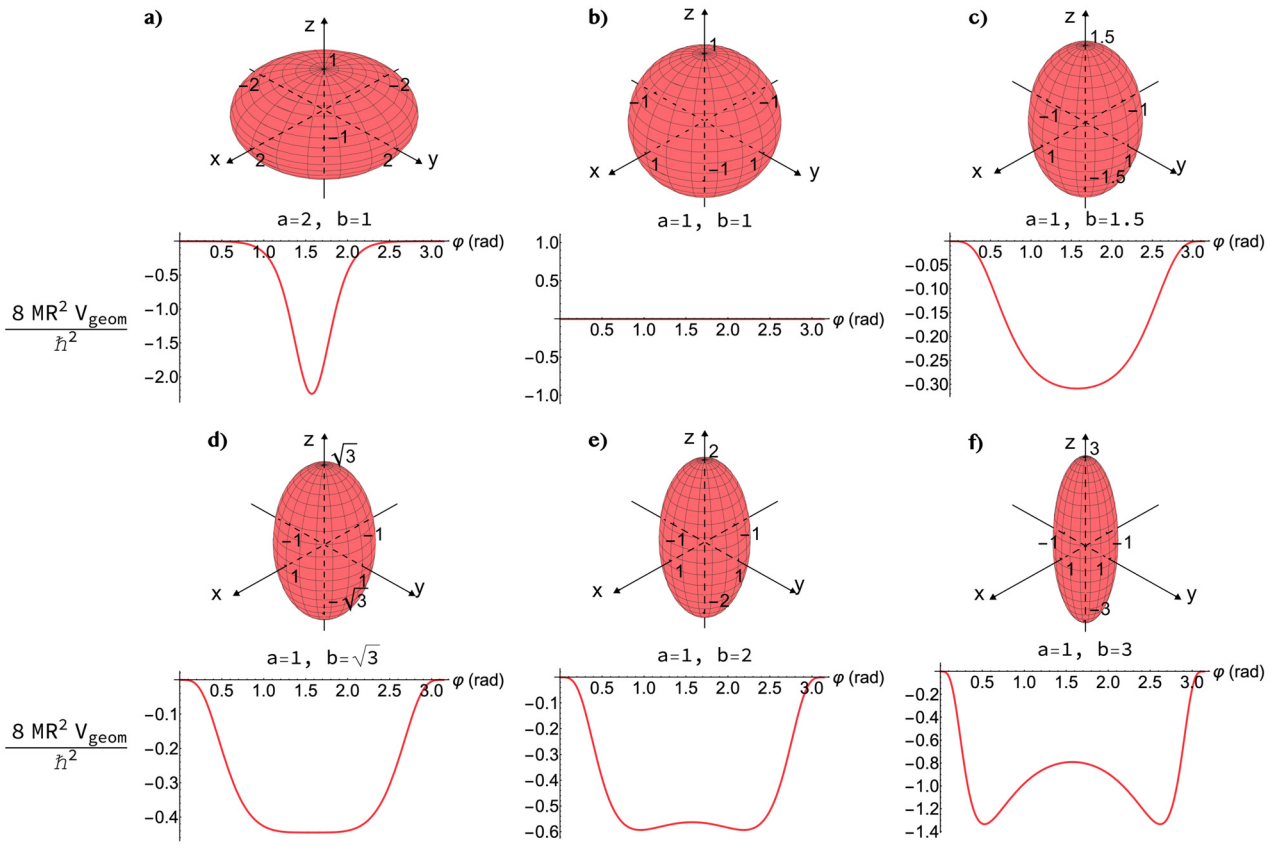

Fig. 1. Geometric potential on ellipsoids for different values of a and b. Oblate ellipsoid: (a) $a=2$ and $b=1$; sphere: (b) $a=b=1$; prolate ellipsoid: (c) $a=1$ and $b=1.5$; (d) $a=1$ and $b=\sqrt{3}$; (e) $a=1$ and $b=2$; and (f) $a=1$ and $b=3$.

of the geometric potential with respect to φ, for different values of a and b.

For $a > b$, we have an oblate ellipsoid and the minimum of the potential is always on $\varphi = \pi/2$, that is, on the equator of the ellipsoid. For $a = b$, we have the special case of a sphere, where the geometric potential vanishes, since $\kappa_1 = \kappa_2$ everywhere. For $b > a$, we have a prolate ellipsoid, and a minimum appears on the equator for $b/a \leq \sqrt{3}$, and a local maximum for $b/a > \sqrt{3}$. Notably, for any value of the ratio between a and b, a global maximum appears on the poles.

Finally, the ground state of the BEC trapped in such an ellipsoid with $\omega_2 = 0$ is given by

$$|\phi_0|^2 = \frac{1}{g_{2D}}\left(\mu_2 + \frac{\hbar^2}{8mR^2}\frac{b^2(a^2-b^2)^2\sin^4\varphi}{a^2(a^2\cos^2\varphi + b^2\sin^2\varphi)^3}\right). \tag{62}$$

Note that the denominator $a^2\cos^2\varphi + b^2\sin^2\varphi$ is always positive. Since $\sin\varphi$ vanishes for $\varphi = 0, \pi$, we can directly see that the points with the lowest density are the poles of the ellipsoid.

Comparing this result with those from the literature we find a discrepancy. The numerical simulations for a BEC confined on a bubble trap[68] and even the experiments with a thermal Bose gas[34] show a higher accumulation of atoms on the poles of the ellipsoid, while our results show this higher accumulation on the equator. We analyze the reasons for this difference in Sec. VIII.

VIII. GROUND STATE AND COMPARISON TO THE BUBBLE TRAP

There is a discrepancy between the ground state evaluated for the bubble trap and the one we found in Sec. VII. One of the reasons for this is that the potential in the experiments does not satisfy one of our hypotheses: the dominant term ω_0 of the confinement frequency is not constant. To see this, consider the bubble-trap potential, which was derived in Refs. 37 and 38

$$U(x,y,z) = \hbar M_F\Delta\sqrt{\left(\frac{m}{4\hbar\Delta}(\omega_x^2x^2 + \omega_y^2y^2 + \omega_z^2z^2) - 1\right)^2 + \frac{\Omega^2}{\Delta^2}}, \tag{63}$$

which is written as Cartesian coordinates (x, y, z). The parameters Δ, Ω, and m are the detuning of the radio frequency magnetic field, the Rabi frequency between the hyperfine levels, and the atomic mass, respectively, while M_F labels the highest dressed state. Moreover, it is assumed that $\Delta \gg \Omega$.

The minimum of this potential defines an ellipsoid with the equation

$$\omega_x^2x^2 + \omega_y^2y^2 + \omega_z^2z^2 = \frac{4\hbar\Delta}{m}. \tag{64}$$

If $\omega_x = \omega_y$, we obtain a symmetric ellipsoid as in Eq. (57). In this case, we can set

$$a = 1\,, \quad b = \frac{\omega_x}{\omega_z}\,, \text{ and } R = \sqrt{\frac{4\hbar\Delta}{m\omega_x^2}}, \tag{65}$$

and potential (63) can be re-expressed as

$$U(x,y,z) = \hbar M_F\Delta\sqrt{\frac{m\omega_x}{4\hbar\Delta}\left(\frac{x^2}{a^2} + \frac{y^2}{a^2} + \frac{z^2}{b^2} - R^2\right)^2 + \frac{\Omega^2}{\Delta^2}}. \tag{66}$$

In prolate spheroidal coordinates, it can be written as

$$U(r) = \hbar M_F\Delta\sqrt{\frac{m\omega_x}{4\hbar\Delta}(r^2 - R^2)^2 + \frac{\Omega^2}{\Delta^2}}, \tag{67}$$

which can be Taylor expanded as

$$U(r) \simeq \hbar M_F\Omega + \frac{M_F\Delta m\omega_x}{\Omega}(r-R)^2 + \cdots. \tag{68}$$

In Gaussian normal coordinates, potential (63) becomes approximately

$$U(x^0,\varphi) \simeq M_F\hbar\Omega + \frac{m\omega_0^2(\varphi)}{2}(x^0)^2 + \cdots, \tag{69}$$

where

$$\omega_0^2(\varphi) = \frac{2M_F\omega_x}{a^2b^2}\frac{\Delta}{\Omega}(a^2\cos^2\varphi + b^2\sin^2\varphi). \tag{70}$$

This expansion is developed in Appendix F.

Remember that $\Delta \gg \Omega$, thus, we cannot apply the dimensional reduction developed in Secs. III, IV, and V to this kind of potential, since one of our hypotheses is that ω_0 is constant. Note that this is not a specific restriction of our dimensional reduction method. In fact, it is not possible to define a two-dimensional wave function in the limit of a thin surface for this potential (63), except for spheres and small deformations on a sphere,[55] where there is only an infinitesimal difference between the parameters a and b.

Here, we work with an ellipsoid chosen in advance, with a finite difference between the parameters a and b. For this kind of surface, it is not possible to perform a well-defined dimensional reduction considering bubble trap potential (63). Even though, we still can use our methods to find some comparison. Motivated by the formula of Eq. (70), we will consider instead the following confinement:

$$U(x^0,\varphi) = \frac{m[\omega_0 + \omega_2(\varphi)]^2}{2}(x^0)^2 \tag{71}$$

with ω_0 defined as in Sec. III, and

$$\omega_2(\varphi) = \beta\frac{\hbar}{4mR^2}(a^2\cos^2\varphi + b^2\sin^2\varphi), \tag{72}$$

where β is a dimensionless constant, with $\mathcal{O}(\beta) = \mathcal{O}(1)$. Thus, we also have that $\mathcal{O}[\omega_2(\varphi)/\omega_R] = \mathcal{O}(1)$ for all $\varphi \in [0, \pi]$, satisfying the conditions of the method developed in Secs. III, IV, and V.

We can then apply the 2DGP equation for this kind of confinement. The ground state from the Thomas–Fermi solution becomes then

$$|\phi_0|^2 = \frac{1}{g_{2D}}\left(\mu_2 - \beta\frac{\hbar^2}{8mR^2}(a^2\cos^2\varphi + b^2\sin^2\varphi) + \frac{\hbar^2}{8mR^2}\frac{b^2(a^2-b^2)^2\sin^4\varphi}{a^2(a^2\cos^2\varphi + b^2\sin^2\varphi)^3}\right) \tag{73}$$

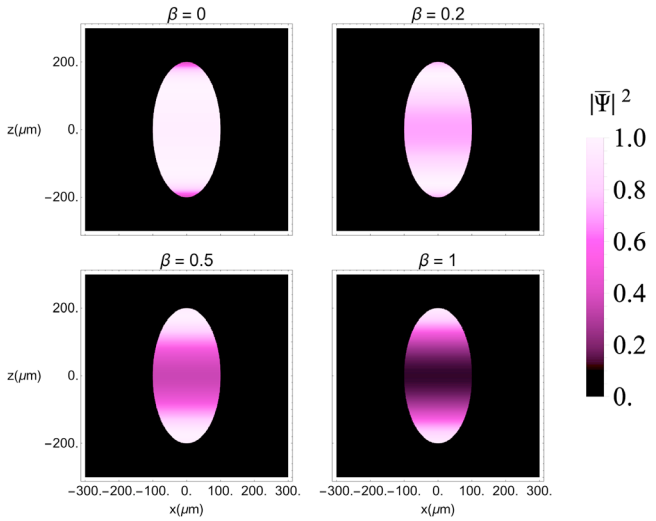

Fig. 2. Profile of the gas density on the ellipsoid surface for different values of β.

We plot the atom density in Fig. 2 for $\beta = 0, 0.2, 0.5$, and 1, considering $a = 1$ and $b = 2$. For $\beta = 0$, we find a higher accumulation of atoms on the equator, that is, at $\varphi = \pi/2$, while for $\beta = 0.5$ and $\beta = 1$, we observe a higher accumulation of atoms on the poles, that is, at $\varphi = 0$ and $\varphi = \pi$. For $\beta = 0.2$, we have an intermediate situation, where the equator and poles both show a higher accumulation in comparison with complementary regions.

To gain a better notion of these differences, we compute the number of atoms on a strip along the equator of angle $\Delta\varphi$, as illustrated in Fig. 3. More precisely, we compute

$$N_{\Delta\varphi} = \int_0^{2\pi} \int_{\frac{\pi-\Delta\varphi}{2}}^{\frac{\pi-\Delta\varphi}{2}} |\phi_0(\varphi)|^2 dA, \tag{74}$$

where θ ranges from 0 to 2π, φ ranges from $(\pi - \Delta\varphi)/2$ to $(\pi + \Delta\varphi)/2$, and $dA = R^2 a \sin\varphi \sqrt{a^2\cos^2\varphi + b^2 \sin^2\varphi}\, d\theta d\varphi$ is the area element.

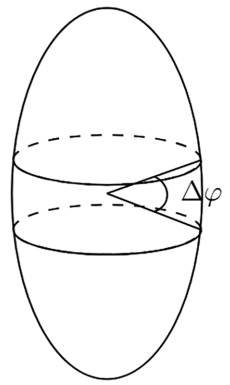

Fig. 3. Strip on an ellipsoid, being defined by $\varphi \in [(\pi - \Delta\varphi)/2, (\pi + \Delta\varphi)/2]$ and $\theta \in [0, 2\pi)$.

We plot this atom number in Fig. 4(a) for the different values of β that we have already considered, where $N = 1000$ is the total atom number. The differences of the atom number in a strip between the uniform case, where $\beta = 0$, and β', for $\beta' = 0.1$, $\beta' = 0.5$ and $\beta' = 1$, is plotted in Fig. 4(b). We see that the biggest differences happen for $\Delta\varphi$ around $\pi/6$ in all three cases, and that they can reach an amount of hundreds of atoms. This shows that the difference in the atom number for different confinements is eligible to be experimentally measured.

IX. DISCUSSION

As we have shown in Sec. VIII, it is not possible to implement a uniform two-dimensional confinement with bubble-trap potential (63), since its asymmetry diverges in the thin limit confinement. On the one hand, without a significant modification to the current techniques to realize a bubble trap, it would be quite challenging to observe the geometric properties of the ground state of a gas confined to the surface of an ellipsoid. On the other hand, these asymmetries could be quite useful for different purposes. For instance, in Ref. 53, the asymmetries are conveniently employed in the realization of a Bose gas on an oblate ellipsoid in a terrestrial laboratory. These asymmetries lead

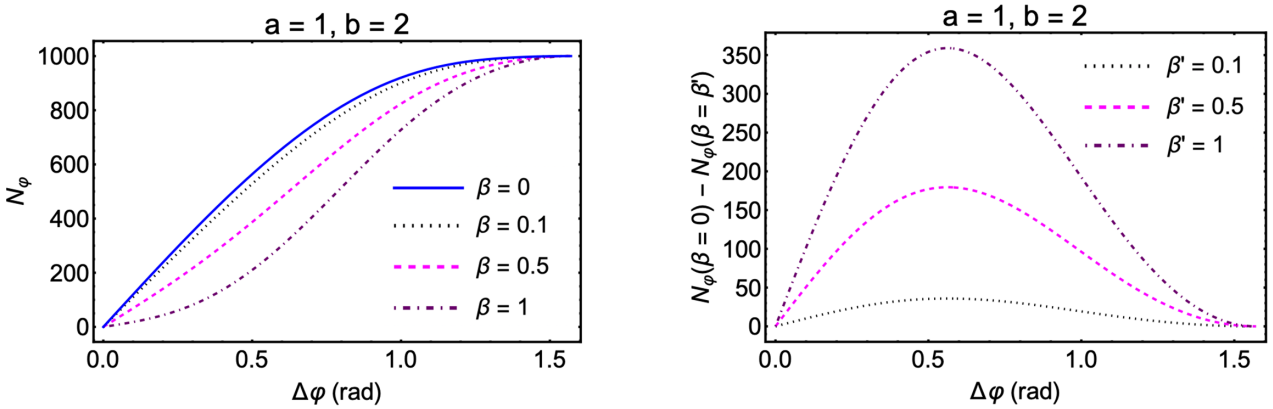

Fig. 4. (a) Number of atoms for different values of β in the interval $\Delta\varphi$. (b) Difference on the atom number between $\beta = 0$ and β' in the interval $\Delta\varphi$, for different values of β'.

to an effective potential on a quasi 2D bubble and are strong enough to partially compensate the gravitational sag effect.

However, a conceptual understanding of geometric effects in a bubble trap is still lacking. For instance, Ref. 52 mentions possible effects of curvature on an ellipsoid, stating that the curvature can lead to local confinement of atoms near the higher curvature regions. Even though this statement is not strictly incorrect, it deserves caution.

According to the analysis we performed here, for an oblate ellipsoid, geometric effects indeed lead to a higher accumulation in the region of higher Gaussian curvature, which is the equator. This can be checked considering Eq. (62), with $a > b$, or simply noticing Fig. 1(a). This coincidence happens in this particular case because the region of higher curvature is the same as the region of higher difference between the principal curvatures.

However, for a prolate ellipsoid, which is the case we focused on in this paper, we have the opposite behavior. The regions of higher Gaussian curvature are the poles, while the region of higher atomic accumulation due to geometric effects is the equator. This contrasts with the inference mentioned above from Ref. 52.

We recall that the word *curvature* is generally used to denote the Gaussian curvature, introduced in Eq. (2), which can also be referred to as *intrinsic curvature*. This curvature receives considerably more attention than the mean and principal curvatures, introduced in Eqs. (1) and (3), which can also be referred to as *extrinsic curvatures*. The reason for this is that, as a consequence of the *Gauss' Egregium Theorem*,[82] the Gaussian curvature is an intrinsic two-dimensional geometric property of a surface.

For instance, one can consider only the inner angles of a local triangle to compute the Gaussian curvature at a point. In particular, if their sum is equal to π, then the Gaussian curvature vanishes and the surface is locally flat at that point. If their sum is larger than π, then the curvature is positive, and if it is smaller than π, the curvature is negative. In contrast, calculating the principal and mean curvatures requires taking into account the three-dimensional space in which the surface is embedded. For instance, one must examine how the normal vector to a surface varies along a path on this same surface. By analyzing the variation of normal vectors, we are inherently accessing three-dimensional properties of the Euclidean space.

We observe that the geometric potential in Eq. (53) depends on the principal curvatures, and consequently, the ground state (56) also depends on them. The effects found here are understood as geometric effects of a surface, which is a two-dimensional manifold embedded in a three-dimensional space. Although it is correct to interpret the gas as occupying a two-dimensional region in the limit of a thin shell, where $\sigma_0 \to \infty$, it still exhibits properties of a system that resides in a three-dimensional space.

X. CONCLUSIONS

In this paper, we unravel the geometric meaning of the ground state of a BEC confined on a surface. To do that, we compute the ground state using a perturbative expansion to the first orders of magnitude of the width of the surface, followed by dimensional reduction techniques. While one can find a term in the expression of the ground state density that appears exclusively due to the curvatures of the surface, there is also another term that does not depend directly on the geometry, but on the asymmetries of confinement. These asymmetries depend on the engineering used to create the confinement potential and might indirectly depend on the geometry due to technical reasons.

In particular, we show that the accumulation of atoms on the poles of a bubble trap happens to be exactly the latter case. It depends on the experimental techniques used and not on the geometrical properties of an ellipsoid. Instead, we show that if these technical asymmetries were eliminated or at least made weaker, it would be possible to observe an accumulation of atoms on the equator of an ellipsoid. This latter accumulation happens exclusively due to the geometric properties of this surface.

The methods used in this paper for deriving the 2DGP equation are elementary, being necessary only differential and integral calculus and basic knowledge of the Dirac delta function distribution. While Ref. 54 considers the minimization principles for Action and Energy, here we only need to assume that the GP equation holds.

For solving the 2DGP equation, we used the Thomas–Fermi approximation, which suits well for our model, since the two-dimensional interactions $g_{2D} = g_{\text{int}}/\left(2\sqrt{2}\,\sigma_0\right)$ are strong for small σ_0. Remember that our results are valid in the regime where the thickness of the cloud gas around the surface is much smaller than its dimensions, which is formally expressed as $\sigma_0 \ll R$. To achieve our main results, we consider the limit $\sigma_0/R \to 0$ and focused on the conceptual geometrical aspects. However, for experimental implementations, it would be valuable to numerically solve the three-dimensional GP equation for different ratios of σ_0/R. This would help assess the limitations of our approximations under realistic experimental conditions.

Our findings also open several promising avenues in theoretical research. A key contribution of the 2DGP equation presented here is the decomposition of the effective potential into two distinct components: the geometric potential and the external potential. A similar decomposition has been developed to gases confined in one dimension, with various applications already explored.[32,89] Our formulation now enables the extension of these insights to systems confined in two dimensions.

Another promising direction involves examining the role of the Laplace–Beltrami operator, $\Delta_{\mathcal{M}}$, in both the ground state and the dynamics of a Bose–Einstein condensate (BEC) uniformly confined on an ellipsoidal surface. For ellipsoids with small deformations (i.e., when $a \simeq b$), it may be possible to adapt the analytical techniques developed in recent work[80] to effectively handle this operator. Finally, further interesting applications of our results can be explored by considering different geometries, such as cylindrical and toroidal shapes,[79,89,90] or even adapting them to deal with non-orientable surfaces, like a Möbius strip.[91]

ACKNOWLEDGMENTS

S.M.O. acknowledges the funding support from DAAD-CAPES, project PROBAL 88887.899314/2023-00, and FAPESP, project 2020/05057-4. N.S.M. acknowledges the support of R2 fellowship for excellent researchers funded by the EU NextGenerationEU through the Recovery and Resilience Plan for Slovakia under the project No. 09I03-03-V04-00679 (INDORABLE), as well as additional support from APVV-22-0570 (DeQHOST) and VEGA 2/0164/25 (QUAS). N.S.M. has benefited from the activities of COST Action CA23115: Relativistic Quantum Information, funded by COST (European Cooperation in Science and Technology).

S.M.O. and N.S.M. thank Axel Pelster for the valuable discussions and for his support throughout all stages of this work. S.M.O. thanks F. Ednilson A. dos Santos for all the support during the development of this work. The authors acknowledge Hélène Perrin for useful discussions.

AUTHOR DECLARATIONS

Conflict of Interest

The authors have no conflicts to disclose.

Author Contributions

Sheilla M. de Oliveira: Formal analysis (equal); Investigation (equal); Methodology (equal); Writing – original draft (equal); Writing – review & editing (equal). **Natália Salomé Móller:** Conceptualization (lead); Formal analysis (equal); Investigation (equal); Methodology (equal); Supervision (lead); Writing – original draft (equal); Writing – review & editing (equal).

DATA AVAILABILITY

Data sharing is not applicable to this article as no new data were created or analyzed in this study.

APPENDIX A: JUSTIFICATION FOR THE TERM $\mu_1 = 0$

In the main text, we obtained Eq. (36), which can be re-expressed as

$$\frac{\partial S_1}{\partial x^0} = \frac{\partial \ln \sqrt{(\det g)^{-1/2}}}{\partial x^0} + \frac{\mu_1 m \sigma_0^2}{\hbar^2 x^0}. \tag{A1}$$

Integrating on x^0, we obtain

$$S_1 = \ln \sqrt{(\det g)^{-1/2}} + \frac{\mu_1 m \sigma_0^2}{\hbar^2} \ln |x^0| + \overline{S_1}(x^1, x^2), \tag{A2}$$

where $\overline{S_1}(x^1, x^2)$ is a parameter that is constant with respect to x^0. Remember that $\ln|x^0|$ diverges for $x^0 \to 0$, which means that the factor S_1 would diverge on the surface. Since this solution has no physical meaning, we must set $\mu_1 = 0$.

APPENDIX B: GAUSSIAN DISTRIBUTIONS AND DIRAC DELTA FUNCTION

Here, we express well-known integrals of a Gaussian distribution, which is the square of the Gaussian wave-function (32), and of this Gaussian distribution times a polynomial.[92] We use it to derive Eq. (45) of the main text.

Indeed, one can show that

$$\int_{-\infty}^{\infty} \mathcal{G}^2(x^0) dx^0 = 1. \tag{B1}$$

Moreover, for a natural even number n, we have that

$$\int_{-\infty}^{\infty} (x^0)^n \mathcal{G}^2(x^0) dx^0 = (n-1)!! \frac{\sigma_0^n}{2^{n/2}}, \tag{B2}$$

while for n odd, we have that

$$\int_{-\infty}^{\infty} (x^0)^n \mathcal{G}^2(x^0) dx^0 = 0. \tag{B3}$$

The integration limit in the above equations ranges from $-\infty$ to ∞, while in the main text, the integrations were evaluated from $-R/2$ to $R/2$. Since we are considering $\sigma_0 \ll R$, we have approximately that[92]

$$\int_{-R/2}^{R/2} (x^0)^n \mathcal{G}^2(x^0) dx^0 = (n-1)!! \frac{\sigma_0^n}{2^{n/2}} + \mathcal{O}(e^{-R/\sigma_0}) \tag{B4}$$

for n even, and

$$\int_{-R/2}^{R/2} (x^0)^n \mathcal{G}^2(x^0) dx^0 = 0 + \mathcal{O}(e^{-R/\sigma_0}) \tag{B5}$$

for n odd.

Now we are going to show that Eq. (45) is indeed valid. Let $\delta_\varepsilon(x^0)$ be a family of integrable functions. We say that

$$\lim_{\varepsilon \to 0} \delta_\varepsilon(x^0) = \delta(x^0), \tag{B6}$$

where $\delta(x^0)$ is the Dirac delta, if and only if

$$\lim_{\varepsilon \to 0} \int_{\mathcal{N}\{x^0=0\}} f(x^0) \delta_\varepsilon(x^0) dx^0 = f(0) \tag{B7}$$

for all well-behaved functions $f(x^0)$, where $\mathcal{N}\{x^0 = 0\}$ is a neighborhood around $x^0 = 0$. As in the main text, for simplicity, we consider that $\mathcal{N}\{x^0 = 0\} = [-R/2, R/2]$. Remember that the Dirac delta is not a function, and that limit (B6) is not rigorously a limit, but a convention of notation. With this convention, let us show that $\lim_{\sigma_0 \to 0} [(x^0)^2/\sigma_0^2] \mathcal{G}^2 = \delta(x^0)/2$, i.e., that Eq. (45) holds.

Considering the Taylor expansion of a well-behaved function $f(x^0)$ around $x^0 = 0$, we can write that

$$\int_{-R/2}^{R/2} f(x^0) \frac{(x^0)^2}{\sigma_0^2} \mathcal{G}^2(x^0) = \sum_{n=0}^{\infty} \frac{f^{(n)}(0)}{n!\,\sigma_0^2} \int_{-R/2}^{R/2} (x^0)^{n+2} \mathcal{G}^2(x^0) dx^0. \tag{B8}$$

From Eqs. (B4) and (B5), it becomes

$$\begin{aligned} &= \sum_{n\text{even}} \frac{(n+1)!!}{n!\, 2^{(n+2)/2}} f^{(n)}(0) \sigma_0^n + \mathcal{O}(e^{-R/\sigma_0}) \\ &= \frac{f(0)}{2} + \frac{3}{8} f''(x^0) \sigma_0^2 + \cdots \end{aligned} \tag{B9}$$

From the above equation, we can see that its limit when $\sigma_0 \to 0$ is equal to $f(0)/2$. With this result and the definition (B6) and (B7), we guarantee the validity of Eq. (45).

APPENDIX C: JUSTIFICATION FOR THE VANISHING OF S_2-INVOLVED TERMS AFTER INTEGRATION

In Sec. IV, we mentioned that the terms associated with S_2 vanish within the range we are considering. In this appendix, we provide the calculations supporting this assertion. However, for a clearer understanding, we recommend reading this appendix after completing Sec. V.

The terms that would appear in the GP equation (27) associated with S_2 that are of order $\mathcal{O}(1)$, are

$$-\frac{\hbar}{2m}(2S_0' S_2' + S_2''). \tag{C1}$$

This is because, according to the hypotheses imposed to the Ansatz (23), we have that $\mathscr{O}(S_0' S_2') = \mathscr{O}([\sigma_0/R]^{-1} \cdot [\sigma_0/R]) = \mathscr{O}(1)$ and $\mathscr{O}(S_2'') = \mathscr{O}(1)$.

Following the methods performed in Secs. IV and V, we need to show that

$$\lim_{\sigma_0 \to 0} \int_{-R/2}^{R/2} (2S_0 S_2' + S_2'') \mathscr{G}^2 dx^0 = 0. \tag{C2}$$

From Eq. (33), we have that

$$2S_0 S_2' + S_2'' = -\frac{2x^0 S_2'}{\sigma_0^2} + S_2''. \tag{C3}$$

Let us consider that S_2 can be Taylor expanded around $x^0 = 0$. With this, we have that S_2 is a sum of terms involving $(x^0)^n$, $n \in \mathbb{N}$. If we show that

$$\lim_{\sigma_0 \to 0} \int_{-R/2}^{R/2} \left(-\frac{2x^0}{\sigma_0^2} ([x^0]^n)' + ([x^0]^n)'' \right) \mathscr{G}^2 dx^0 = 0, \tag{C4}$$

then we guarantee that Eq. (C2) holds. Evaluating the above expression, we have that

$$\lim_{\sigma_0 \to 0} \int_{-R/2}^{R/2} \left(-\frac{2n(x^0)^n}{\sigma_0^2} + n(n-1)(x^0)^{n-2} \right) \mathscr{G}^2 dx^0. \tag{C5}$$

From Eq. (B4), we evaluate that the above becomes approximately

$$\lim_{\sigma_0 \to 0} \left(-\frac{2n(n-1)!! \sigma_0^n}{2^{n/2} \sigma_0^2} + \frac{n(n-1)(n-3)!! \sigma_0^{n-2}}{2^{(n-2)/2}} \right), \tag{C6}$$

and we can directly check that the terms inside the parentheses vanish, as we would like to show.

With this, we conclude that the terms that appear in the three-dimensional GP equation that are associated with S_2, vanish in the 2DGP equation up to order $\mathscr{O}(1)$.

APPENDIX D: THE GAUSSIAN NORMAL COORDINATE SYSTEM FOR A PROLATE ELLIPSOID

In this appendix, we show how to transform between the Cartesian, prolate spheroidal, and Gaussian normal coordinate systems, with the surface $\mathscr{M}$ being the prolate ellipsoid defined in Eq. (57).

To work on these formulas, we initially express a generic point $\mathbf{q}$ and the point $\mathbf{p}$ on the ellipsoid, which is the closest one to $\mathbf{q}$ on this surface. Due to the symmetry of the prolate ellipsoid, we have that the angle θ in prolate spheroidal coordinates (58) for both $\mathbf{p}$ and $\mathbf{q}$ is the same. Without loss of generality, we can consider that $\theta = 0$ (equivalently, $y = 0$) and work only on the plane defined by this constraint (equivalently, plane $x - z$). Figure 5 illustrates this ellipse, which is the intersection of the original ellipsoid and the plane $x - z$, together to and the points $\mathbf{p}$ and $\mathbf{q}$.

For the point $\mathbf{p}$, in the modified spherical coordinates we have $r = R$ and in the Gaussian normal coordinates we have $x^0 = 0$. With that said, denote the Cartesian coordinates of $\mathbf{p}$ and $\mathbf{q}$ as (x_p, z_p) and (x, z), the modified spherical coordinates as (R, φ) and $(r, \overline{\varphi})$, and the Gaussian normal coordinate system as $(0, \varphi)$ and (x^0, φ), respectively. Note that in the Gaussian normal coordinate system, we are choosing $x^2 = \theta$, see Fig. 5 for an illustration of these coordinates. For simplicity, we are hiding the third coordinate in all the cases, that is, we will omit y, θ, and x^2. Due the above discussion, we were free to set conveniently the values of y and θ, and the same argument holds to x^2.

From the definition of the Gaussian normal coordinate system, we have the relation

$$\mathbf{q} = \mathbf{p} + x^0 \mathbf{n}, \tag{D1}$$

where $\mathbf{n}$ is the normal vector to the ellipsoid at the point $\mathbf{p}$. This expression can be visualized in Fig. 5.

Note that we can express the variables from different coordinate systems as

$$\begin{aligned} x_p &= Ra \sin\varphi \quad x = ra \sin\overline{\varphi}, \\ z_p &= Rb \cos\varphi \quad z = rb \cos\overline{\varphi}. \end{aligned} \tag{D2}$$

The normal vector $\mathbf{n} = (n_x, n_y)$ can be computed as the following. It is orthogonal to the tangent vector $\partial\mathbf{p}/\partial\varphi$ to $\mathbf{p}$. Using the above equation, we can compute that $\partial\mathbf{p}/\partial\varphi = (Ra\cos\varphi, -Rb\sin\varphi)$. From the relation $\mathbf{n} \cdot \partial\mathbf{p}/\partial\varphi = 0$, we obtain that

$$\mathbf{n} = \frac{(b\sin\varphi, a\cos\varphi)}{\sqrt{a^2\cos^2\varphi + b^2\sin^2\varphi}} = \frac{(b^2 x_p, a^2 z_p)}{\sqrt{a^4 z_p^2 + b^4 x_p^2}}. \tag{D3}$$

Expressing $\mathbf{p}$, $\mathbf{q}$, and $\mathbf{n}$ in Cartesian coordinates, relation (D1) becomes

$$(x, z) = (x_p, z_p) + x^0 \frac{(b^2 x_p, a^2 z_p)}{\sqrt{a^4 z_p^2 + b^4 x_p^2}}. \tag{D4}$$

Using relations (D2), we obtain

$$\begin{aligned} (ra\sin\overline{\varphi}, rb\cos\overline{\varphi}) = (Ra\sin\varphi, Rb\cos\varphi) \\ + x^0 \frac{(b\sin\varphi, a\cos\varphi)}{\sqrt{a^2\cos^2\varphi + b^2\sin^2\varphi}}. \end{aligned} \tag{D5}$$

We divide the first component of the above vector by a and the second one by b. Summing up the squared of these two terms yields to

$$\begin{aligned} r^2 = R^2 + \frac{2x^0 R}{ab} \sqrt{a^2\cos^2\varphi + b^2\sin^2\varphi} \\ + \frac{(x^0)^2}{a^2 b^2} \frac{a^4\cos^2\varphi + b^4\sin^2\varphi}{a^2\cos^2\varphi + b^2\sin^2\varphi}. \end{aligned} \tag{D6}$$

From the two above Eqs. (D5) and (D6), we obtain r and $\overline{\varphi}$ from x^0 and φ. That is, once one knows the coordinates of a point in the Gaussian normal coordinate system, one can obtain its coordinates in the prolate spheroidal coordinate system. From Eqs. (D2), one can then obtain the coordinates of this point in the Cartesian coordinate system.

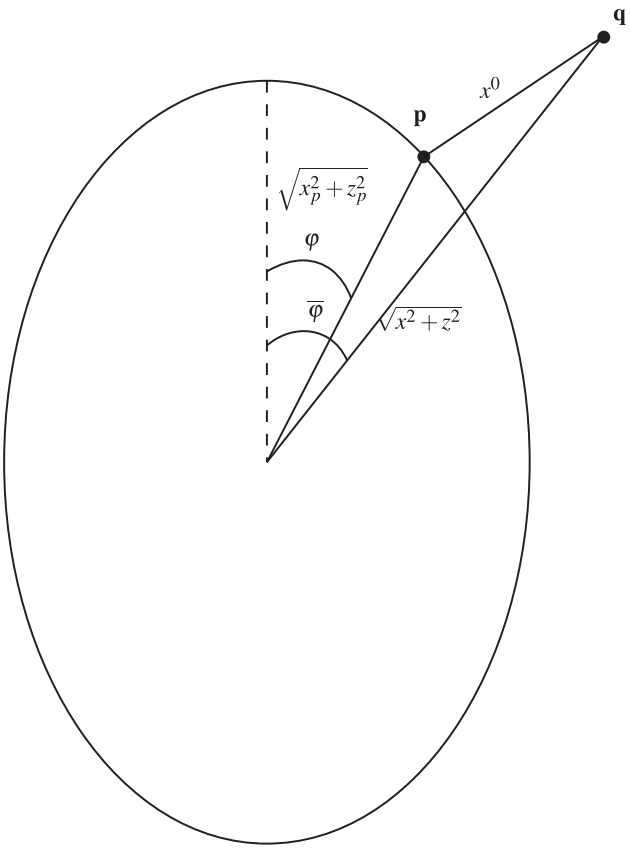

Cartesian:

$$\mathbf{p}=(x_p,z_p) \qquad \mathbf{q}=(x,z)$$

Prolate spheroidal:

$$\mathbf{p}=(R,\varphi) \qquad \mathbf{q}=(r,\overline{\varphi})$$

Gaussian normal:

$$\mathbf{p}=(0,\varphi) \qquad \mathbf{q}=\left(x^0,\varphi\right)$$

Fig. 5. Cartesian, prolate spheroidal and Gaussian normal coordinate systems represented on the plane with constant θ for the points $\mathbf{q}$ and $\mathbf{p}$. The point $\mathbf{p}$ lies on a prolate ellipsoid and is the nearest point on this surface to the point $\mathbf{q}$.

Now, to obtain the coordinates of a point once one knows it in the Cartesian, or prolate spheroidal coordinate systems, it is necessary to invert these equations. From the Cartesian to the prolate spheroidal coordinate system, we have that

$$r=\sqrt{\frac{x^2}{a^2}+\frac{z^2}{b^2}}, \tag{D7}$$

and $\overline{\varphi}$ must satisfy

$$\cos\overline{\varphi}=\frac{x}{ar} \quad \text{and} \quad \sin\overline{\varphi}=\frac{z}{br}. \tag{D8}$$

Now, to obtain the coordinates in the Gaussian normal coordinate system, we can proceed as the following. From Eq. (D5), we can re-express

$$x^0=\sqrt{a^2\cos^2\varphi+b^2\sin^2\varphi}\,\frac{(ra\sin\overline{\varphi}-Ra\sin\varphi)}{b\sin\varphi} \tag{D9}$$

and

$$x^0=\sqrt{a^2\cos^2\varphi+b^2\sin^2\varphi}\,\frac{(rb\cos\overline{\varphi}-Rb\cos\varphi)}{a\cos\varphi}. \tag{D10}$$

Comparing these two equations, we find that

$$\frac{b\cos\overline{\varphi}}{a\cos\varphi}+\frac{R}{r}\left(\frac{a}{b}-\frac{b}{a}\right)=\frac{a\sin\overline{\varphi}}{b\sin\varphi}. \tag{D11}$$

By squaring this equation and replacing $\sin^2\varphi$ by $1-\cos^2\varphi$, we obtain $\cos\varphi$ as one of the roots of the fourth-degree polynomial

$$\begin{aligned} &b^4\cos^2\overline{\varphi}-\frac{2Rb^2}{r}(b^2-a^2)\cos\overline{\varphi}\cos\varphi \\ &+\left(\frac{R^2(b^2-a^2)^2}{r^2}-\left[b^4\cos^2\overline{\varphi}+a^4\sin^2\overline{\varphi}\right]\right)\cos^2\varphi \\ &+\frac{2Rb^2}{r}(b^2-a^2)\cos\overline{\varphi}\cos^3\varphi-\frac{R^2(b^2-a^2)^2}{r^2}\cos^4\varphi=0. \end{aligned} \tag{D12}$$

The solution for $\cos\varphi$ as one of the roots of the above polynomial is a function of the ellipsoid parameters a, b, and R, and of the prolate spheroidal coordinates $\overline{r}$ and $\overline{\varphi}$. For instance, for $r=1$, $a=1$, $b=1.5$, only two of the four roots are real numbers. One of them corresponds to the parameters of the closest point and the other to the furthest one. One can use Eq. (D9) to determine x^0 and choose the smallest value, and from this, determine the correspondent φ.

Note, however, that x^0 is the distance from a point to the ellipsoid. With this in mind, one can have a better visualization of the

ellipsoid's properties in this coordinate system than one would obtain by looking at the method we above described.

APPENDIX E: THE UNIFORM CONFINEMENT POTENTIAL

A uniform confinement has a very simple expression in the Gaussian normal coordinate system, given by

$$V = \frac{m\omega^2}{2}(x^0)^2, \tag{E1}$$

which correspond to Eq. (15) for $\omega_2 = 0$.

However, it is not so simple to be expressed in the prolate spheroidal and in the Cartesian coordinate systems. In these coordinates, the variable x^0 is expressed as a function of r and $\overline{\varphi}$, and of x and z, respectively. However, to explicitly write this dependence, one must solve the fourth-degree polynomial (D12) and follow the procedure explained in Appendix D. The roots of a fourth-degree polynomial exist, their expressions are analytic and are easily solvable via numeric methods. However, the resulting expressions are lengthy and impractical for manual manipulation. Because of this complexity, in this paper, we restrict the explicit expression of the uniform confinement potential to the above expression (E1).

APPENDIX F: THE BUBBLE TRAP POTENTIAL EXPRESSED IN THE GAUSSIAN NORMAL COORDINATE SYSTEM

The confinement potential of a bubble trap is given in Eqs. (66) and (67) in the Cartesian and prolate spheroidal coordinate systems, respectively, and, approximately, in Eqs. (68) and (69) in the Gaussian normal coordinate system.

This expression in Cartesian coordinates is obtained in the literature, and the one in prolate spheroidal coordinate was obtained with algebraic manipulation in the main text. However, obtaining the bubble trap potential in the Gaussian normal coordinate system is more elaborated, being necessary to solve the fourth degree polynomial (D12) for an analytic expression. Thus, we simply obtained an approximation of this potential in these coordinates. To do that, we perform a Taylor expansion of equations around $x^0 = 0$ on Eq. (D6)

$$r \simeq R + \frac{x^0}{ab}\sqrt{a^2\cos^2\varphi + b^2\sin^2\varphi} + \frac{(x^0)^2}{2Ra^2b^2}\left(\frac{a^4\sin^2\varphi + b^4\cos^2\varphi}{a^2\sin^2\varphi + b^2\cos^2\varphi} - (a^2\sin^2\varphi + b^2\cos^2\varphi)\right) + \cdots. \tag{F1}$$

Then, we can approximate

$$(r-R)^2 \simeq \frac{(a^2\cos^2\varphi + b^2\sin^2\varphi)}{ab}(x^0)^2 + \cdots. \tag{F2}$$

Inserting this expression into Eq. (68), we obtain (69) and (70), which is the bubble trap potential expressed in the Gaussian normal coordinate system.

REFERENCES

[1] B. S. DeWitt, Rev. Mod. Phys. **29**, 377 (1957).
[2] H. Jensen and H. Koppe, Ann. Phys. **63**, 586 (1971).
[3] R. da Costa, Phys. Rev. A **23**, 1982 (1981).
[4] P. Gentile, M. Cuoco, O. M. Volkov, Z.-J. Ying, I. J. Vera-Marun, D. Makarov, and C. Ortix, Nat. Electron. **5**, 551 (2022).
[5] R. Streubel, P. Fischer, F. Kronast, V. P. Kravchuk, D. D. Sheka, Y. Gaididei, O. G. Schmidt, and D. Makarov, J. Phys. D **49**, 363001 (2016).
[6] A. Szameit, F. Dreisow, M. Heinrich, R. Keil, S. Nolte, A. Tünnermann, and S. Longhi, Phys. Rev. Lett. **104**, 150403 (2010).
[7] M. Zheng, A. Jagota, E. D. Semke, B. A. Diner, R. S. McLean, S. R. Lustig, R. E. Richardson, and N. G. Tassi, Nat. Mater. **2**, 338 (2003).
[8] A. Tononi and L. Salasnich, Nat. Rev. Phys. **5**, 398 (2023).
[9] I. Bloch, J. Dalibard, and W. Zwerger, Rev. Mod. Phys. **80**, 885 (2008).
[10] A. Görlitz, J. Vogels, A. Leanhardt, C. Raman, T. Gustavson, J. Abo-Shaeer, A. Chikkatur, S. Gupta, S. Inouye *et al.*, Phys. Rev. Lett. **87**, 130402 (2001).
[11] D. Rychtarik, B. Engeser, H.-C. Nägerl, and R. Grimm, Phys. Rev. Lett. **92**, 173003 (2004).
[12] N. D. Mermin and H. Wagner, Phys. Rev. Lett. **17**, 1133 (1966).
[13] P. C. Hohenberg, Phys. Rev. **158**, 383 (1967).
[14] V. Bagnato and D. Kleppner, Phys. Rev. A **44**, 7439 (1991).
[15] M. Olshanii, Phys. Rev. Lett. **81**, 938 (1998).
[16] A. Jackson, G. Kavoulakis, and C. Pethick, Phys. Rev. A **58**, 2417 (1998).
[17] M. L. Chiofalo and M. Tosi, Phys. Lett. A **268**, 406 (2000).
[18] L. Salasnich, A. Parola, and L. Reatto, Phys. Rev. A **65**, 043614 (2002).
[19] S. Gupta, K. Murch, K. Moore, T. Purdy, and D. Stamper-Kurn, Phys. Rev. Lett. **95**, 143201 (2005).
[20] C. Ryu, M. Andersen, P. Clade, V. Natarajan, K. Helmerson, and W. D. Phillips, Phys. Rev. Lett. **99**, 260401 (2007).
[21] W. Heathcote, E. Nugent, B. Sheard, and C. Foot, New J. Phys. **10**, 043012 (2008).
[22] B. Sherlock, M. Gildemeister, E. Owen, E. Nugent, and C. Foot, Phys. Rev. A **83**, 043408 (2011).
[23] A. Ramanathan, K. Wright, S. R. Muniz, M. Zelan, W. Hill III, C. Lobb, K. Helmerson, W. Phillips, and G. Campbell, Phys. Rev. Lett. **106**, 130401 (2011).
[24] S. Moulder, S. Beattie, R. P. Smith, N. Tammuz, and Z. Hadzibabic, Phys. Rev. A **86**, 013629 (2012).
[25] C. Ryu, K. Henderson, and M. Boshier, New J. Phys. **16**, 013046 (2014).
[26] S. Schwartz, M. Cozzini, C. Menotti, I. Carusotto, P. Bouyer, and S. Stringari, New J. Phys. **8**, 162 (2006).
[27] S. Eckel, J. G. Lee, F. Jendrzejewski, N. Murray, C. W. Clark, C. J. Lobb, W. D. Phillips, M. Edwards, and G. K. Campbell, Nature **506**, 200 (2014).
[28] D. Gallucci and N. Proukakis, New J. Phys. **18**, 025004 (2016).
[29] A. V. Yulin, Y. V. Bludov, V. V. Konotop, V. Kuzmiak, and M. Salerno, Phys. Rev. A **84**, 063638 (2011).
[30] S. Eckel, A. Kumar, T. Jacobson, I. B. Spielman, and G. K. Campbell, Phys. Rev. X **8**, 021021 (2018).
[31] K. Henderson, C. Ryu, C. MacCormick, and M. Boshier, New J. Phys. **11**, 043030 (2009).
[32] L. Salasnich, SciPost Phys. Core **5**, 015 (2022).
[33] P. Sandin, M. Ögren, M. Gulliksson, J. Smyrnakis, M. Magiropoulos, and G. Kavoulakis, Phys. Rev. E **95**, 012142 (2017).
[34] R. A. Carollo, D. C. Aveline, B. Rhyno, S. Vishveshwara, C. Lannert, J. D. Murphree, E. R. Elliott, J. R. Williams, R. J. Thompson *et al.*, Nature **606**, 281 (2022).
[35] F. Jia, Z. Huang, L. Qiu, R. Zhou, Y. Yan, and D. Wang, Phys. Rev. Lett. **129**, 243402 (2022).
[36] O. Zobay and B. Garraway, Acta Phys. Slovaca **50**, 359 (2000).
[37] O. Zobay and B. M. Garraway, Phys. Rev. Lett. **86**, 1195 (2001).
[38] O. Zobay and B. M. Garraway, Phys. Rev. A **69**, 023605 (2004).
[39] Y. Colombe, B. Mercier, H. Perrin, and V. Lorent, J. Phys. IV **116**, 247 (2004).
[40] Y. Colombe, E. Knyazchyan, O. Morizot, B. Mercier, V. Lorent, and H. Perrin, Europhys. Lett. **67**, 593 (2004).
[41] B. M. Garraway and H. Perrin, J. Phys. B **49**, 172001 (2016).
[42] H. Perrin and B. M. Garraway, "Trapping atoms with radio frequency adiabatic potentials," in *Advances in Atomic, Molecular, and Optical Physics* (Elsevier, 2017), Vol. 66, pp. 181–262.

[43]E. R. Elliott, M. C. Krutzik, J. R. Williams, R. J. Thompson, and D. C. Aveline, npj Microgravity **4**, 16 (2018).
[44]N. Lundblad, "Microgravity dynamics of bubble-geometry Bose–Einstein condensates," in *NASA Space Life and Physical Sciences Research and Applications Division Task Book* (NASA, 2017).
[45]N. Lundblad, R. Carollo, C. Lannert, M. Gold, X. Jiang, D. Paseltiner, N. Sergay, and D. Aveline, npj Microgravity **5**, 30 (2019).
[46]K. Frye, S. Abend, W. Bartosch, A. Bawamia, D. Becker, H. Blume, C. Braxmaier, S.-W. Chiow, M. A. Efremov *et al.*, EPJ Quantum Technol. **8**, 1 (2021).
[47]D. C. Aveline, J. R. Williams, E. R. Elliott, C. Dutenhoffer, J. R. Kellogg, J. M. Kohel, N. E. Lay, K. Oudrhiri, R. F. Shotwell *et al.*, Nature **582**, 193 (2020).
[48]T.-L. Ho and V. Shenoy, Phys. Rev. Lett. **77**, 3276 (1996).
[49]H. Pu and N. Bigelow, Phys. Rev. Lett. **80**, 1130 (1998).
[50]A. Wolf, P. Boegel, M. Meister, A. Balaž, N. Gaaloul, and M. A. Efremov, Phys. Rev. A **106**, 013309 (2022).
[51]N. Lundblad, D. C. Aveline, A. Balaž, E. Bentine, N. P. Bigelow, P. Boegel, M. A. Efremov, N. Gaaloul, M. Meister *et al.*, Quantum Sci. Technol. **8**, 024003 (2023).
[52]R. Dubessy and H. Perrin, AVS Quantum Sci. **7**, 010501 (2025).
[53]Y. Guo, E. M. Gutierrez, D. Rey, T. Badr, A. Perrin, L. Longchambon, V. S. Bagnato, H. Perrin, and R. Dubessy, New J. Phys. **24**, 093040 (2022).
[54]N. S. Móller, F. E. A. dos Santos, V. S. Bagnato, and A. Pelster, New J. Phys. **22**, 063059 (2020).
[55]E. J. Biral, N. S. Móller, A. Pelster, and F. E. A. dos Santos, New J. Phys. **26**, 013035 (2024).
[56]C. Lannert, T.-C. Wei, and S. Vishveshwara, Phys. Rev. A **75**, 013611 (2007).
[57]K. Sun, K. Padavić, F. Yang, S. Vishveshwara, and C. Lannert, Phys. Rev. A **98**, 013609 (2018).
[58]K. Padavić, K. Sun, C. Lannert, and S. Vishveshwara, Europhys. Lett. **120**, 20004 (2017).
[59]P. C. Diniz, E. A. Oliveira, A. R. Lima, and E. A. Henn, Sci. Rep. **10**, 4831 (2020).
[60]S. J. Bereta, L. Madeira, V. S. Bagnato, and M. A. Caracanhas, Am. J. Phys. **87**, 924 (2019).
[61]A. Tononi and L. Salasnich, Phys. Rev. Lett. **123**, 160403 (2019).
[62]B. Rhyno, N. Lundblad, D. C. Aveline, C. Lannert, and S. Vishveshwara, Phys. Rev. A **104**, 063310 (2021).
[63]A. Tononi, A. Pelster, and L. Salasnich, Phys. Rev. Res. **4**, 013122 (2022).
[64]S. Prestipino and P. V. Giaquinta, Phys. Rev. A **99**, 063619 (2019).
[65]M. Ciardi, F. Cinti, G. Pellicane, and S. Prestipino, Phys. Rev. Lett. **132**, 026001 (2024).
[66]A. Andriati, L. Brito, L. Tomio, and A. Gammal, Phys. Rev. A **104**, 033318 (2021).
[67]L. Brito, L. Tomio, and A. Gammal, Phys. Rev. A **108**, 053315 (2023).
[68]A. Tononi, F. Cinti, and L. Salasnich, Phys. Rev. Lett. **125**, 010402 (2020).
[69]M. Meister, A. Roura, E. M. Rasel, and W. P. Schleich, New J. Phys. **21**, 013039 (2019).
[70]S. K. Adhikari, Phys. Rev. A **85**, 053631 (2012).
[71]M. Arazo, R. Mayol, and M. Guilleumas, New J. Phys. **23**, 113040 (2021).
[72]J. Sánchez-Baena, R. Bombín, and J. Boronat, Phys. Rev. Res. **6**, 033116 (2024).
[73]S. J. Bereta, M. A. Caracanhas, and A. L. Fetter, Phys. Rev. A **103**, 053306 (2021).
[74]K. Padavić, K. Sun, C. Lannert, and S. Vishveshwara, Phys. Rev. A **102**, 043305 (2020).
[75]H. Saito and M. Hayashi, J. Phys. Soc. Jpn. **92**, 044003 (2023).
[76]C. M. Carmesin and M. A. Efremov, "Confinement induced resonances in spherical shell traps," Phys. Rev. Lett. **134**, 243401 (2025).
[77]A. Tononi, Phys. Rev. A **105**, 023324 (2022).
[78]A. Tononi and L. Salasnich, Phys. Rep. **1072**, 1 (2024).
[79]A. Tononi and G. Astrakharchik, "Bose-Einstein condensation on axially-symmetric surfaces," Phys. Rev. A **112**, 023302 (2025).
[80]J. Yi, W. Zhang, R. Zhang, and T. Shi, Europhys. Lett. **150**, 55001 (2025).
[81]C. Lämmerzahl, Phys. Lett. A **203**, 12 (1995).
[82]M. P. Do Carmo, *Differential Geometry of Curves and Surfaces: Revised and Updated*, 2nd ed. (Courier Dover Publications, 2016).
[83]J. M. Lee, *Riemannian Manifolds: An Introduction to Curvature* (Springer Science & Business Media, 2006), Vol. 176.
[84]J. Jost and J. Jost, *Riemannian Geometry and Geometric Analysis* (Springer, 2008), Vol. 42005.
[85]J. A. Smoller and B. Temple, Arch. Ration. Mech. Anal. **128**, 249 (1994).
[86]M. Z. Iofa, Adv. High Energy Phys. **2016**, 5632734.
[87]P. Hartman and A. Wintner, Am. J. Math. **75**, 298 (1953).
[88]G. B. Arfken and H.-J. Weber, Complex Var. **224**, 370 (2003).
[89]Y. Nikolaieva, L. Salasnich, and A. Yakimenko, New J. Phys. **25**, 103003 (2023).
[90]A. Tononi, L. Salasnich, and A. Yakimenko, AVS Quantum Sci. **6**, 030502 (2024).
[91]H.-B. Luo, G. Li, F.-Q. Dou, B. Liu, B. A. Malomed, J. Batle, and Y. Li, Phys. Rev. A **111**, 023325 (2025).
[92]I. S. Gradshteyn and I. M. Ryzhik, *Table of Integrals, Series, and Products* (Academic Press, 2014).